Analysis of Magnetic Anomalies in Determining Fault Displacement in the Crystalline Precambrian Basement underneath the Bellefontaine Outlier, Ohio.

Senior Thesis

Submitted in Partial Fullfillment of the Requirements
for the Degree of Bachelor of Science
in Geological Sciences

By

Kelley J. Kaltenbach

The Ohio State University
Spring Quarter 1998

Approved by:

Dr. Hallan C. Noltimier

Acknoledgements

This senior thesis has much of its roots in the previous research of others. I would like to thank Christian Steck for his valuable input to this project. I would also like to extend a thanks to the members of the Cincinnati Arch Consortium for their efforts in researching the East Continental Rift Basin and other aspects of Ohio geology. The Ohio Division of Geological Survey also served as an important resource of information, and I thank them as well. I would also like to thank John Weaver for his intensive work on the Bellefontaine Outlier, Ohio. Without his hard work and valuable field data, none of this would be possible.

I owe a debt of gratitude to my advisor Dr. Hallan Noltimier, who oversaw the growth and development of this thesis and myself as a geologist. Dr. Noltimier gave me crucial information and helpful advice, which made writing this paper a satisfying experience.

Finally I want to thank my family and friends for their continual support. Without it, I would have left spinning my wheels in the dust and not have gone anywhere.

It is my sincere hope that my thesis will help shed some light into the mysterious realm of the Precambrian and the origin of the Bellefontaine Outlier, Ohio.

Contents

Figures

Tables

Figure 1. **County map of Ohio showing the location of the study area in Champaign and Logan counties. Modified from Steck, 1997.**

Introduction

The Bellefontaine Outlier is located in Logan and Champaign counties of west central Ohio (see figure 1). Topographically, the highest point of the Outlier is located at Campbell Hill, which is also the highest point in Ohio, 1549 ft above sea level. The Bellefontaine Outlier is a highland that rises 500 ft above the surrounding flat glaciated landscape. The rocks of the Outlier are Devonian Shales and carbonates, capped by Pleistocene till. Surrounding the Outlier are older Silurian limestones, dolomites and shales (see figure 2). (Steck, 1996).

The Bellefontaine Outlier was originally interpreted to be a glacial remnant from the Wisconsin Age glaciation. However, after the COCORP OH-1 seismic line was run through Ohio the data revealed a complex basement structure, involving much faulting and the presence of the Grenville Tectonic Front. Lack of deep drilling data has left the origin of the Outlier to subsurface geophysics and well log data. The Paleozoic rocks making up the Outlier overlie the north-south trending Grenville Tectonic Front. East of the Grenville Tectonic Front are Grenville metamorphic granite gneiss, amphibolite, marble, and schist. Precambrian lithic sandstones and felsic volcanics lie to the west (Lucius and Von Frese, 1988). Gravity, magnetic, seismic and limited deep well data have been used to study the basement geology of Ohio. Gravity and magnetic anomaly studies of the region suggest that the Outlier lies on top of a reverse graben, whose displacement may have persisted from the lower Paleozoic to the Recent. It is believed that basement structure plays a key role in the aerial distribution of rocks of the Bellefontaine Outlier. Faulting and resulting reverse graben structures were the chief contributors to the development of the Outlier, rather than random weathering.

My work is a part of a continuing investigation of the Bellefontiane Outlier, began by John Weaver in 1992. Christian Steck continued the work studying gravity anomalies over the region. He used the gravity anomalies to solve for the fault throws of several

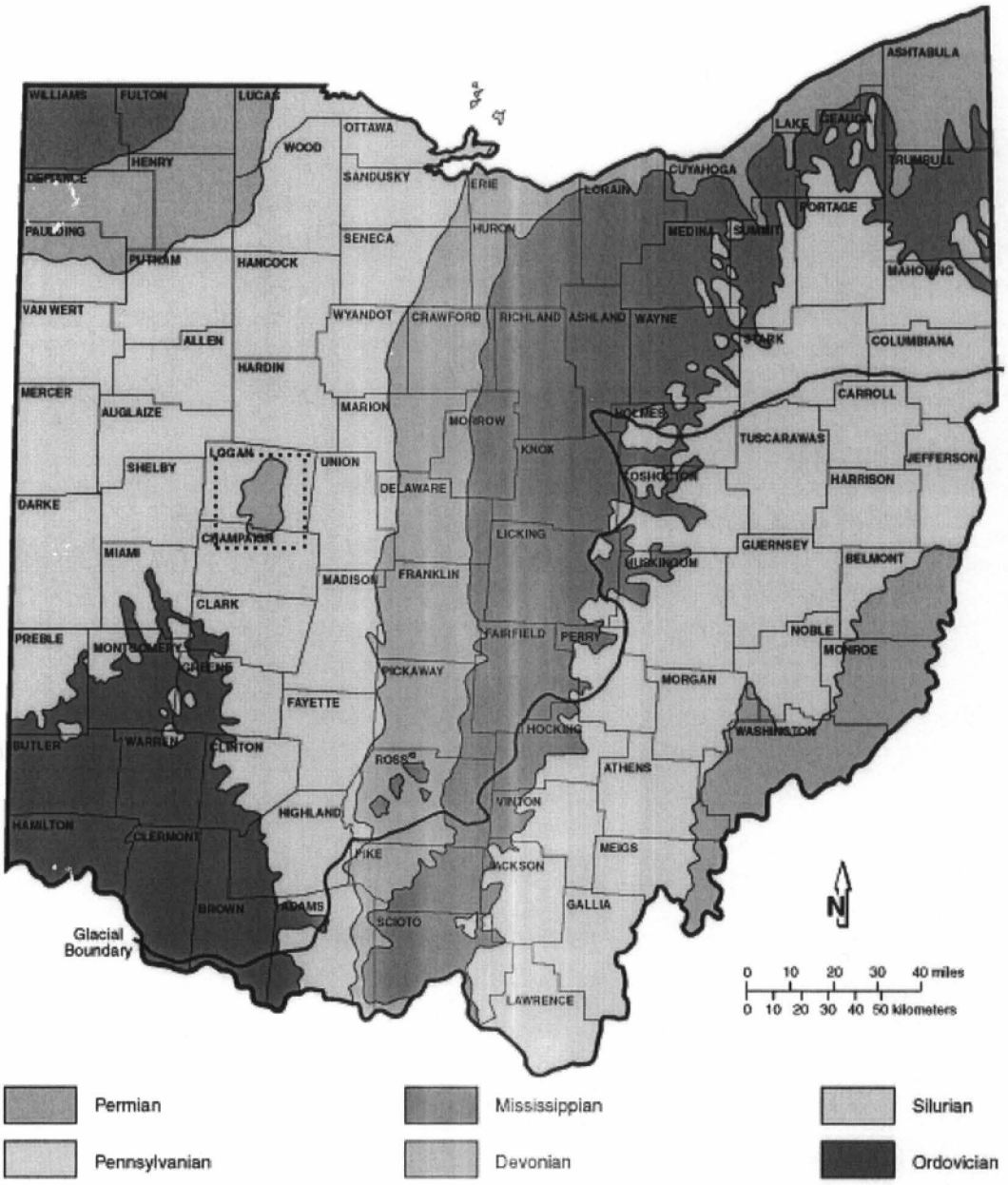

Figure 2. **Geology map of Ohio showing the Bellefontaine Outlier and study area. Modified from the Ohio Geological Survey.**

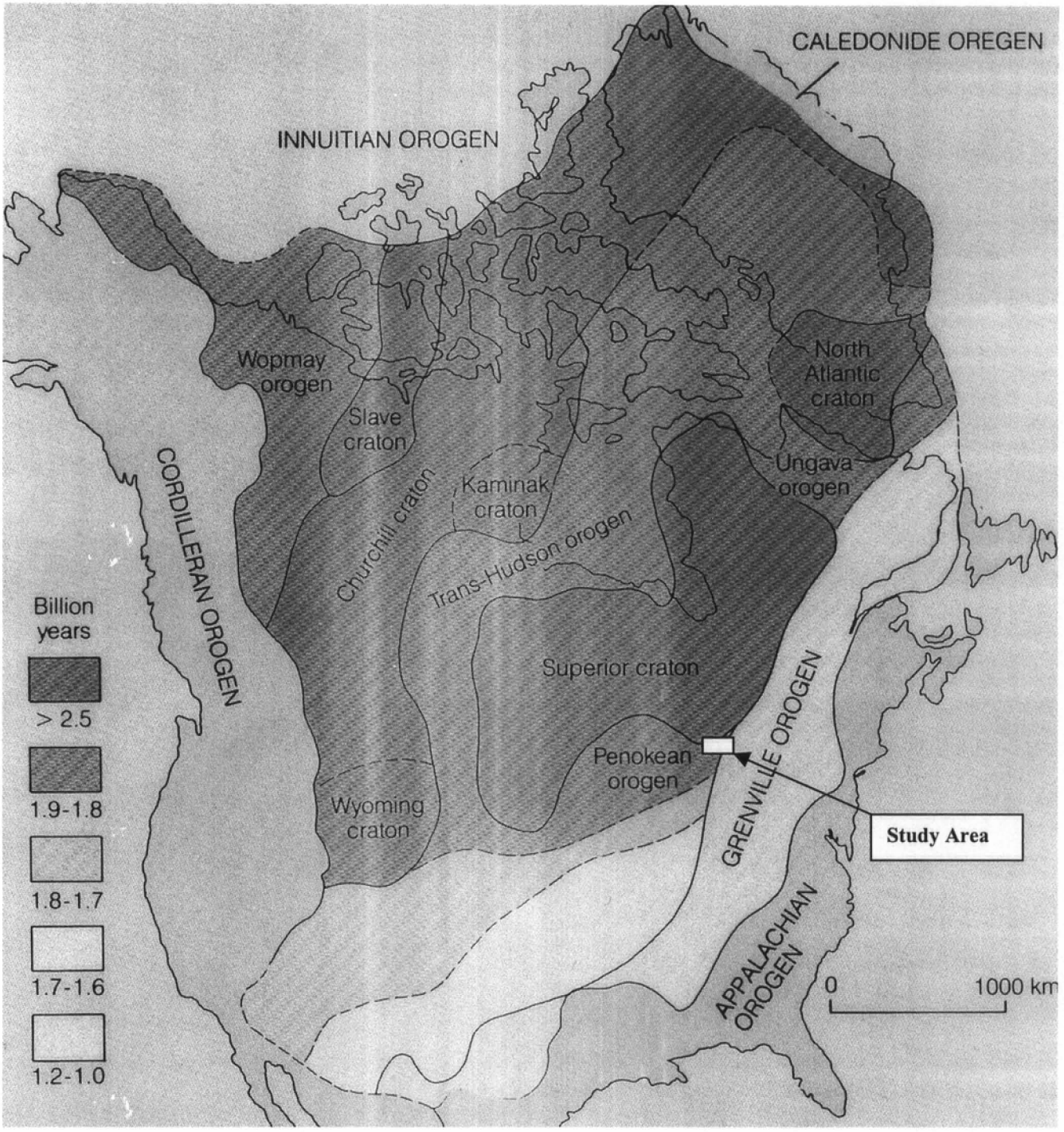

Figure 3. **Map of the various cratons and orogenic belts of North America. Modified from Hoffman, 1988.**

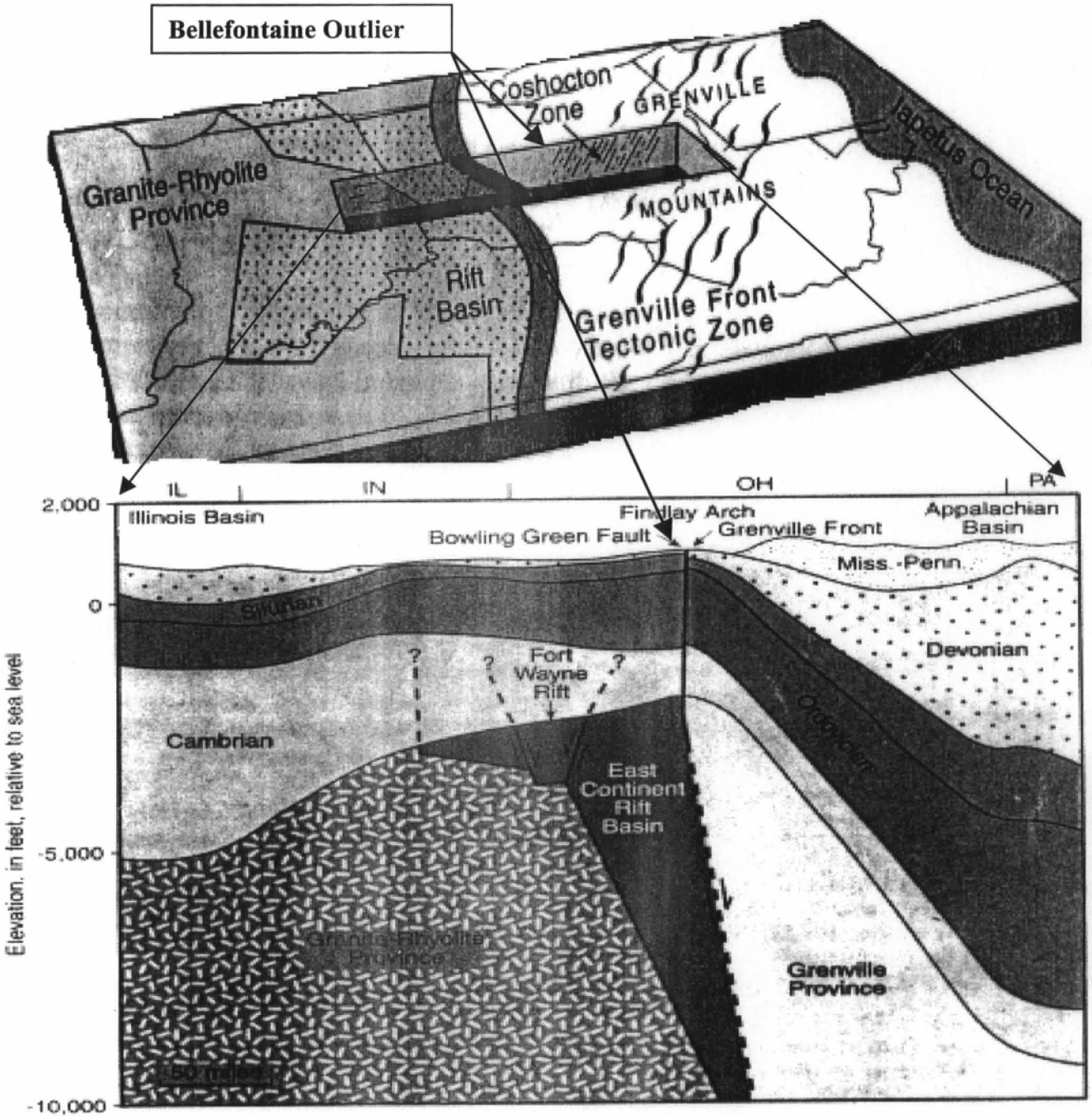

Figure 4. **Diagram of the tectonic setting of the Bellefontaine Outlier and study area within the East Coninental Rift Basin. Modified from Hansen, 1996.**

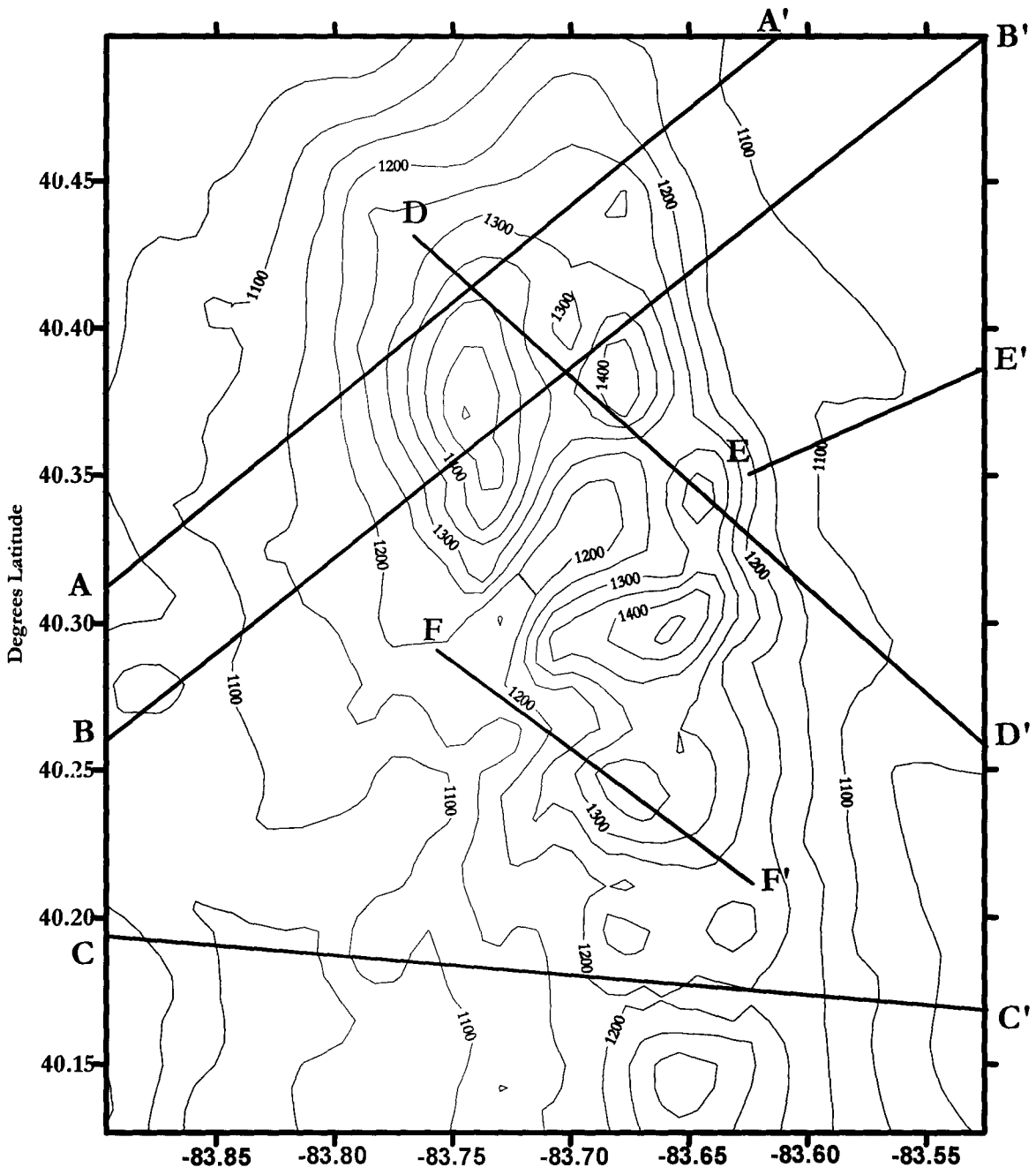

Figure 5. **Topography map of the Bellefontaine Outlier and study area. Modified from Steck, 1996. Contour interval is 50 feet.**

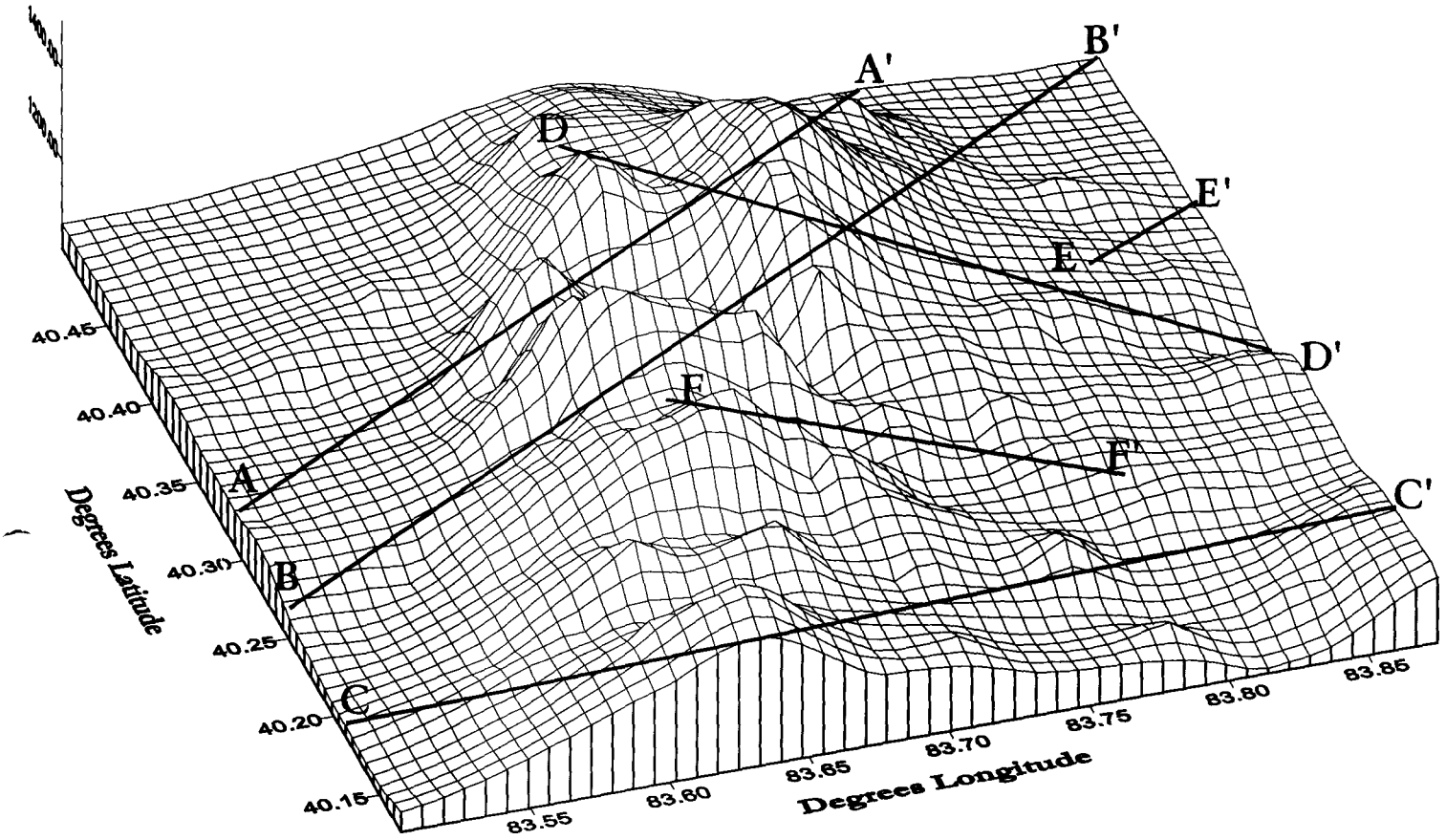

Figure 6. 3-Dimensional topographic map of Bellefontaine Outlier and study area. Vertically exaggerated to show relief.

faults in the basement under the Outlier. I used magnetics to identify those faults found by Steck, and independently solve for their throws. The purpose is to see if the solution based upon the magnetic anomalies would support the gravity interpretation. I also used magnetics to identify faults not picked up by the gravity. A large magnetic anomaly located in the southeastern corner of the study area was also investigated. It is believed that a volcanic plug within the basement complex may produce the anomaly.

Chapter 1: Regional Geology

General Tectonic History

The accretion of exotic terraines (see figure 3) to the North American protocontinent continent of Laurentia began in the Early Proterizoic. The oldest tectonic events under Ohio occurred 1.4 to 1.5 billion years ago, during the Middle Proterozoic. A mantle "super swell" produced a vast field of layered granite and rhyolite seven miles thick (see figures 4 and 7). Named the Granite-Rhyolite Province, it is a prominent feature of the basement geology of Ohio and neighboring western states. The thermal expansion and crustal tension produced by the mantle "super swell" and emplacement of the Granite-Rhyolite Province resulted in faulting and rift basin formation. The rift basin that formed is named the East Continental Rift Basin (ECRB). It is believed that western Ohio was the eastern edge of Laurentia after the Middle Proterozoic. The crustal rifting in Ohio is believed to be similar to a system of faults that extend from Nebraska and Iowa to Lake Superior and northern Michigan. This basement structure is named the Keweenawan Rift System, and it represents the effect of the widespread crustal doming and thermal expansion that occurred during the Mid-Proterozoic. As the rifting continued, the ECRB was gradually filled by erosion of the neighboring basin highlands, basalt flows and volcanic debris. This thick sequence of strata is named the Middle Run Formation. By 1.06 billion years ago, mantle swelling, volcanic activity and basin filling

had ceased. Sediment loading and crustal subsidence had allowed the basin to be filled to 20,000 feet in places (Drahovzal et. al., 1992; Hansen, 1996).

The Grenville Orogeny which is believed to be the result of continental collision involving Laurentia and Baltica occurred roughly 800 to 990 million years ago (see figure 7). The collision is believed to have occurred along a 3000-mile margin of the North American Craton, involving tremendous crustal compression and metamorphism. The Grenville Mountains would have been about the same scale, if not larger, than the present North American Cordillera. What is interpreted to be the main suture zone of the collision between Laurentia and Baltica is believed to lie beneath Coshocton County, Ohio. Deep western dipping reflectors were observed in the COCORP OH-1 Profile across Ohio. The reflectors were interpreted to be a zone roughly oriented north-south and 30 miles wide, consisting of deformed thrust slices dipping to the east (Pratt et.al., 1989). This zone whose western edge lies near the Bellefontaine Outlier, is named the Grenville Front Tectonic Zone. It is believed to represent the western limit of the Grenville Orogeny. (Hansen, 1996).

Following the Grenville Orogeny, a 300 million-year period of deep erosion scoured away much of the Grenville Mountains. The late Precambrian exposed the high-grade metamorphic rocks of the mountain roots and the upper part of the rift basin sedimentary rocks. (Drahovzal, 1992; Hansen, 1996). Transgression of the Iapetus Ocean at the end of the Precambrian Eon influenced sediment deposition over Proterozoic rocks. Several tectonic events influenced the deposition of sediments in Ohio during the Phanerzoic Eon. The Middle-Late Ordovician Taconic Orogeny involved closure of the Iapetus Ocean. Mountain building in New England and New York influenced the deposition of shales and carbonates in Ohio. In the Late Devonian, the closure of the Merrimech Fredricton Ocean and the accretion of the Avalonia terrain to Laurentia marked the Acadian Orogeny. Sediment influx from the Acadian Orogeny led to the deposition of more carbonates and shales. The Alleghenian Orogeny involved the closure

of the Theic-Reiic Ocean and the continental collision between North America and Africa in the Late Carboniferous. This Wilson Cycle event may have influenced the deposition of coal seams in southern and eastern Ohio (Wilson, 1997).

Precambrian Crystalline Basement

The Precambrian basement is the main focus in the gravity and magnetic studies. The basement is the main contributor to the magnetic anomalies involved with the Bellefontaine Outlier. Unfortunately, little is known about the nature of the basement rocks. Over 160 boreholes have been drilled to the basement, yet, only 30 meters or less have been sampled. Geophysical studies are the key tools today in investigating the basement structure. Geophysical data strongly suggest that the study area overlies a complex fault system and the Grenville Tectonic Front Zone. It is believed that there are high angle reverse faults, and reverse grabens within the ECRB (Steck, 1997).

Granite Rhyolite Province

The Granite Rhyolite province is located in western Ohio, and extends from Fulton County in the north to Clermont County in the south. The Proteriozoic Granite Rhyolite Province is a vast body of layered igneous rock 7 miles thick and almost 106 miles wide east to west. It is known to extend across western Ohio, Indiana and Illinois. The COCORP seismic survey OH-1 defines the body as the top of the deepest strong planar continuous reflectors above chaotic reflectors. The seismic study revealed suggestive information that the body was stratified granite-ryholite possibly intermixed with, or underlain by, mafic or sedimentary rocks. (Pratt et. al., 1989). This region is identifiable from the aeromagnetic map produced by Lucius and Von Frese (1988) as an area with broad low amplitude anomalies associated with igneous rocks.

Emplacement of the Granite-Rhyolite Province. A 7 mile thick sheet of granite and rhyolite emplaced by intrusive and extrusive events This event is believed to have been caused by a mantle superswell 1.5 G.a.

B. Keweenawan Rift Event. Thermal expansion from the mantle superswell may have been the driving force to cause doming, normal faulting and rifting. Volcanics and mafic dike emplacement associated with rifting also occurred. Clastic sediments derived from erosion of tilted fault blocks and volcanic debris filled the rift basin. This fill is now known as the Middle Run Formation. 1.0 G.a. rifting stopped, and volcanic activity died, leaving the basin an aborted rift.

C. Overthrusting of Grenville allochthon. Estimated age of event is 990 to 880 M.a. The Grenville Orogeny to the east thrusted Grenvillian rocks westward in decollement sheets over the Keweenawan rocks. This thrusting cut the older Keweenawan rocks and transported the shallower parts of them west. Grenville foreland basin sediments were deposited over the Keweenawan rocks as well.

D. Late Proterizioc erosion and faulting. An extensive period of erosion in the Late Proterizoic scoured the Grenville Mountains down to their deep rooted metamorphic cores. This erosion may have also removed the foreland basin sediments and upper parts of the rift basin. Strike-slip faulting occurred near the Grenville Front destoying some evidence of thrusting. Believed to have occurred 1000 M.a. to 800 M.a., but before 500 M.a.

E. Tectonic stability and transgression of Cambrian seas. Deposition of sediment form Cambrian seas turn the region into a passive margin. Crustal subsidence occurs due to the increased load of sediment. As a result a thick sequence of sedimentary rock is deposited upon the Precambrian rocks.

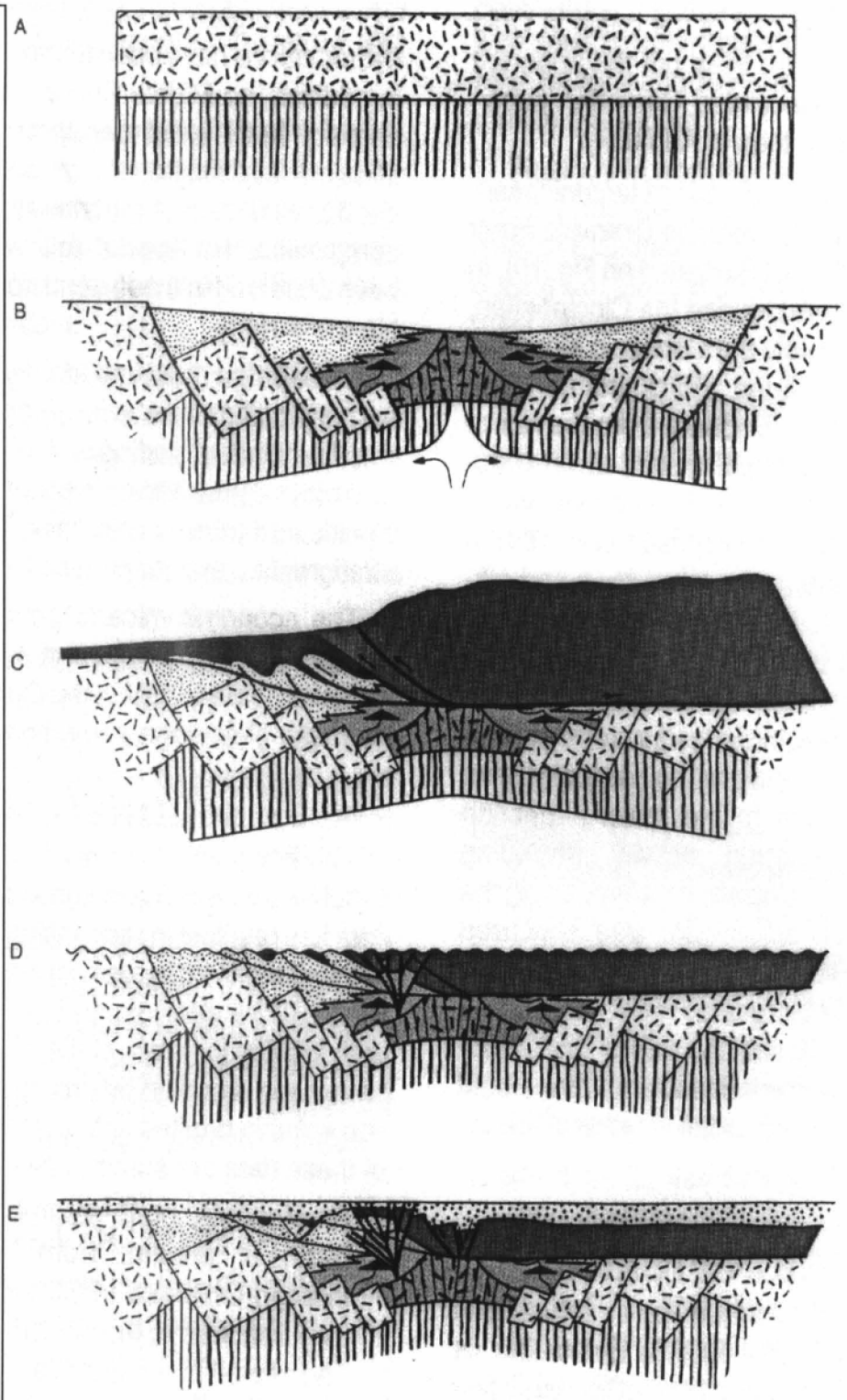

Figure 7. Development of the East Continental Rift Basin. Modified from Drahovzal et.al., 1992.

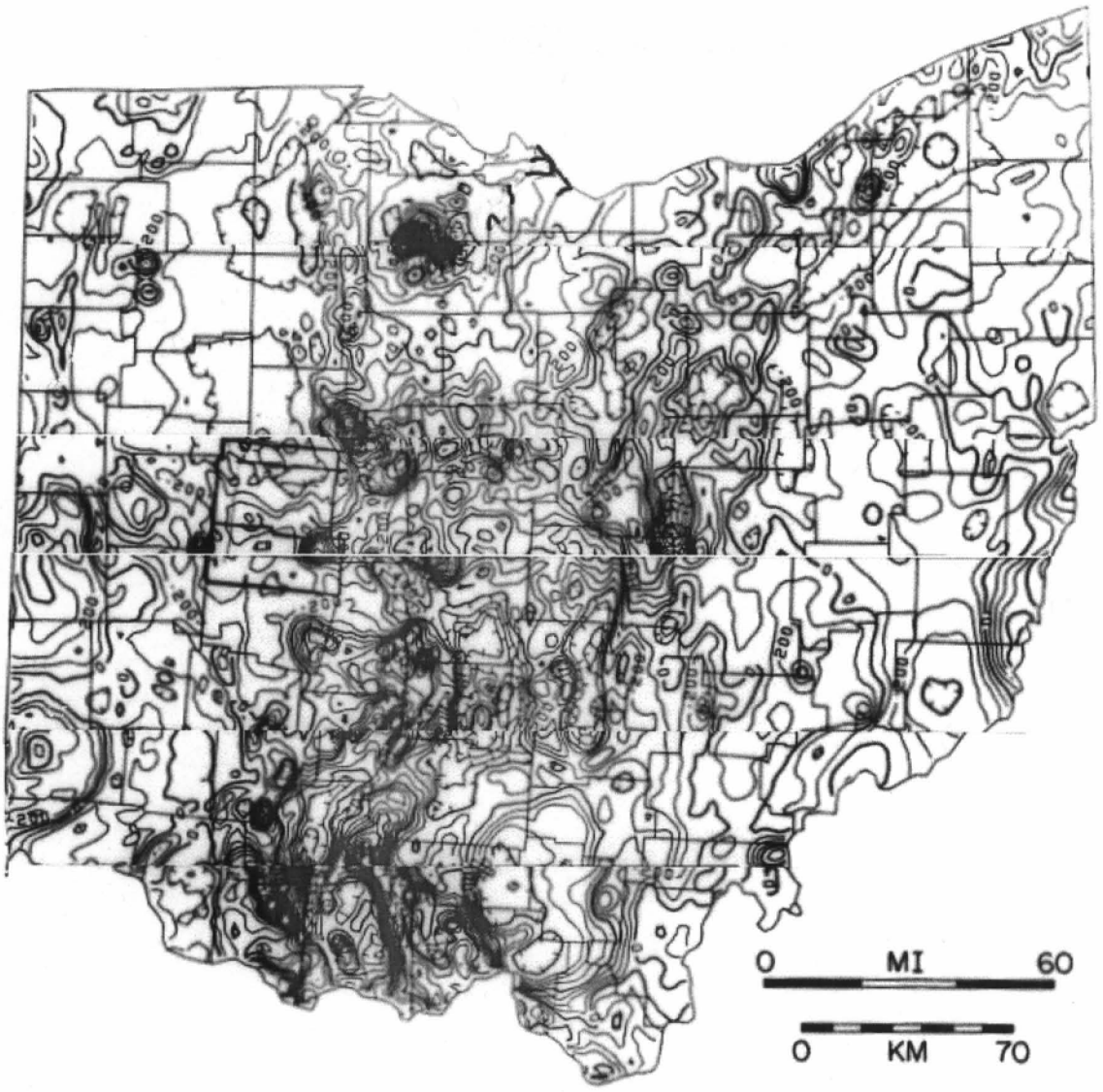

Figure 8. **Aeromagnetic map of Ohio modified from Lucius and Von Frese, 1988. Contour interval is 100 nT. Note the line of high amplitude anomalies that trend north-south through the center of the state. These magnetic demarcate the western boundry of the Grenville Front Tectonic Zone. These anomalies are thought to be produced by either mafic volcanic plugs or ore deposits.**

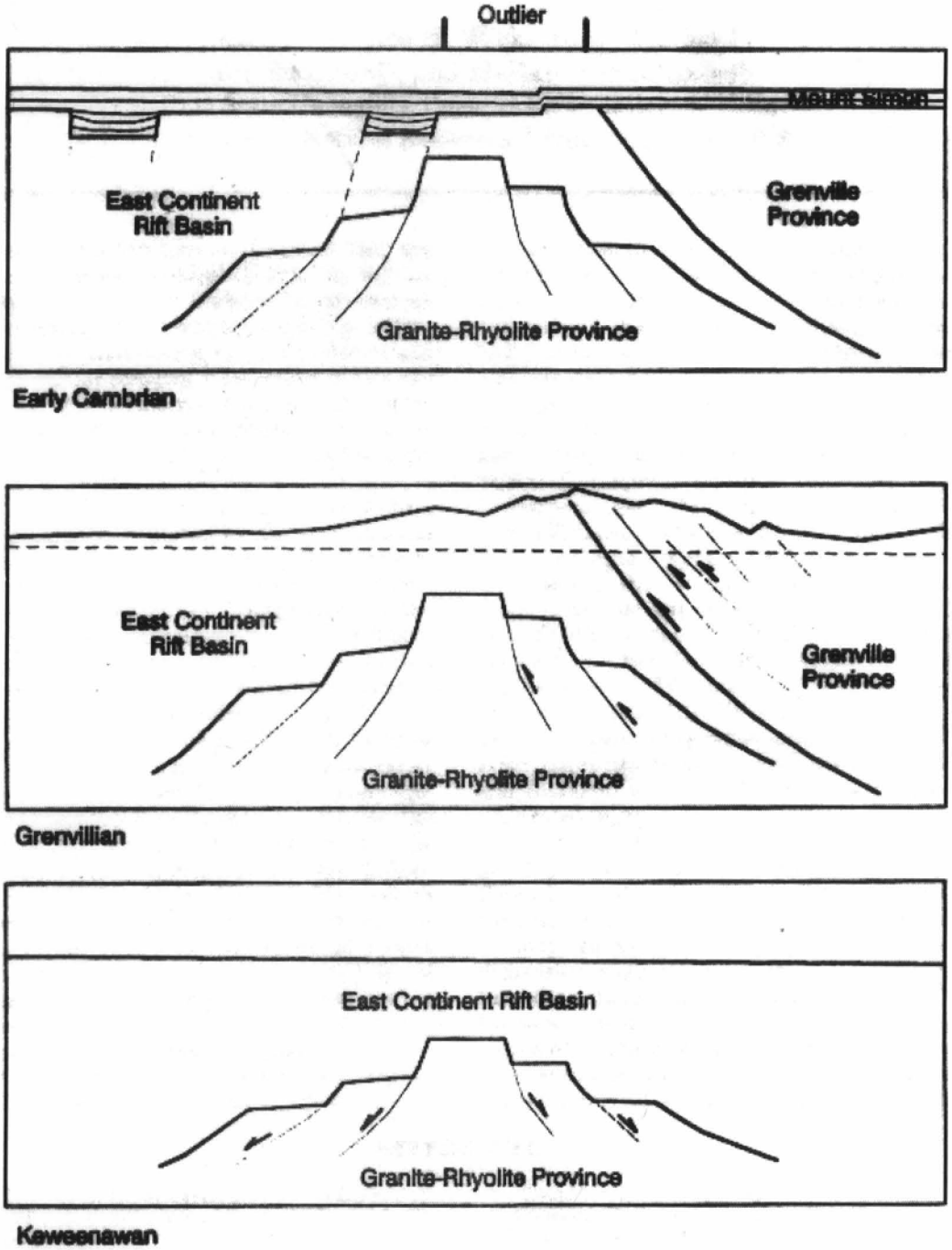

Figure 9. **Sequence of events that led to the basement configuration of the Bellefontaine Outlier. Extension during Keweenawan Rifting produced a reverse graben. Emplacement of the Grenville allocthon produeced the Grenville Front. Sedimentation during the Paleozoic produced thick sedimentary sequence. Modified from Steck et. al., 1997.**

The basement topography of this province dips steeply to the east due to faulting and basin subsidence. The apex of the Granite-Rhyolite Province is approximately -2500 feet elevation, and it plunges to -25,000 feet at the border of the Grenville Front. Within the study area, has a-7500 feet elevation and drops to -15,000 feet at the eastern boundary.

In the study area, the Granite-Rhyolite Province rocks are buried by the Middle Run Formation and volcanic debris associated with the ECRB. The Middle Run Formation is 5000 to 15,000 feet thick as one travels west to east. (Steck, 1996).

East Continental Rift Basin

The ECRB was formed from extension and faulting of the Granite-Rhyolite Province, then the Late Proterizoic crust. As thermal expansion continued the crust was tensionally faulted and thinned. Due to isotacy, the thinner crust was also topographically low, and it became a rift valley that would be subsequently filled by sediment. Sources of sediment would have been clastics from surrounding ridges, and volcanics. This sediment filling is known as the Middle Run Formation. The ECRB extends from the Grenville Front in central Ohio and Kentucky through much of Indiana. The rift basin filling reaches a maximum thickness of 25,000 feet in northwestern Ohio. It ranges in thickness of 3000 feet to 25,000 feet at the Grenville Front. Magnetic modeling and seismicity suggest that the ECRB plunges to -27,000 feet elevation underneath the Cincinnati Arch. Sediment and volcanic debris there is believed to be 22,500 feet thick. The ECRB thins to the west due to uplifting from regional compression. It is believed that the Fort Wayne Rift may divide the ECRB into northern and southern sub-basins. (Steck, 1996). Seismicity indicates that the basin is highly faulted with vertical fault throws as great as 7000 feet. Faulting within the ECRB may be the result of Proterozoic Keweenawan Rifting or the later Grenville compression. The ECRB is thought to be a part of the Keweenawan Rift System as its seismic properties and stratigraphy are similar. In light of

this, the ECRB may link up with the Mid-Continental Rift Basin (MCRB) in Michigan to the north. The southern boundary of the ECRB is thought to extend and narrow into central Tennessee. The western boundary may be limited by the tilted and faulted Granite-Rhyolite Province rocks, or it may extend as far as the Illinois Basin. (Steck,1996).

Grenville Front Tectonic Zone

The Grenville Front Tectonic Zone (GFTZ) is a 2500 mile long structural feature that stretches from the Labrador coast to Lake Huron, then southward through Ohio and beyond. The GFTZ represents the western edge of the Grenville Mountain chain (Hansen, 1989). The approximate position of the GFTZ was determined using seismic, magnetic and borehole data. Grenville Front suture zones and thrust belts have been determined from deep seismic reflectors. The reflectors are east dipping at 28 degrees. The aeromagnetic map produced by Lucius and Von Frese (see figure 8), shows a distinct north-south trending line of high amplitude magnetic anomalies. The line of anomalies extend from Michigan through western Ohio and then south to central Kentucky and Tennessee (see figures 8 and 10). The magnetic and gravity anomalies were interpreted by previous workers to be deep-rooted mafic bodies, possibly emplaced during the Keweenawan Rift event (Drahovzal, 1992). Mafic volcanic basement lithologies were determined to be characteristic of some of the anomalies in west central Ohio (Lucius and Von Frese, 1988). Magnetic signature east of the Grenville Front are not as well defined. Metamorphic rocks yield a lower amplitude magnetic anomaly than basalts or volcanics. This detail has been used to interpret the rifting to be Pre-Grenvillian. Rift associated volcanics were metamorphosed by compression during the Grenville Orogeny. Metamorphosed basalts is believed to be the origin of amphibolites in basement wells east of the Grenville Front in Ohio (Drahovzal, 1992).

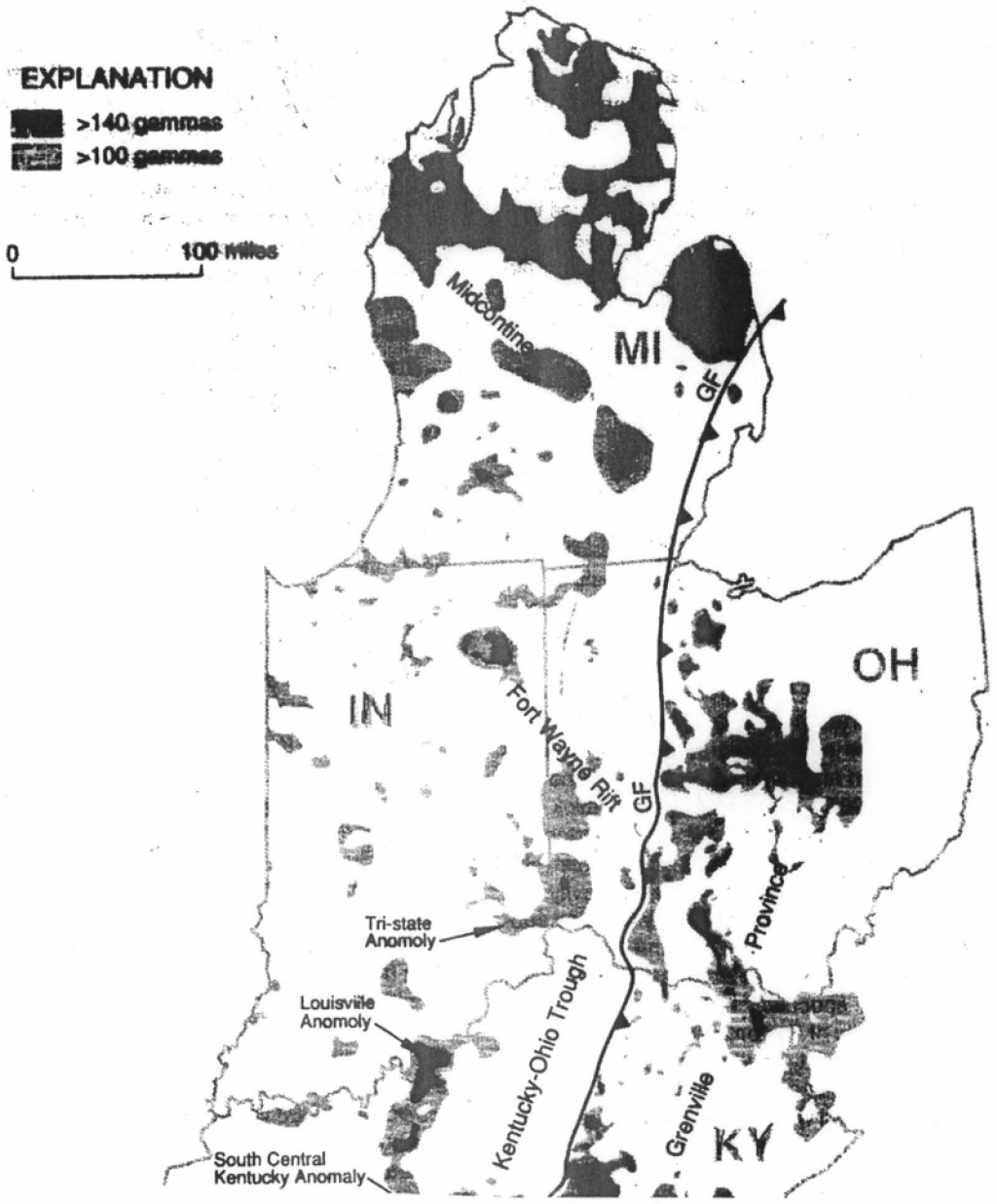

Figure 10. **Regional magnetic map of the west central United States. Note that the magnetic anomalies increase in magnitude near the rift zones and the Grenville Front. Modified from Drahovzal et. al., 1992.**

Grenville Province

Based upon age dating of Grenville rocks, the origin of the Grenville Province and thrust belt occurred 880 to 990 million years ago. The Grenville Province is an extension of the Grenville metamorphic terrain exposed in southern Canada. Grenville Province rocks are considered to be regionally metamorphosed igneous and sedimentary rocks derived from the Proterizoic plate collision that built the Grenville Mountains. Rocks that have been identified in the Grenville province are granite-gneiss, schist, amphibole, charnokite and marble (Drahovzal, 1992; Lucius and Von Frese, 1988). COCORP Seismic line OH-1 revealed that Grenvillian rocks were thrusted and folded against the rocks of the East Continental Rift Basin and the Granite Ryholite Province. Reprocessed COCORP OH-1 data allowed workers to interpret the Grenville Province as the eastern border of the ECRB. The Grenville Province itself is characterized seismically by west dipping reflectors of angles up to 40 degrees. The seismic work revealed a 100-mile wide structural feature, named the Coshocton Zone. (Pratt et al., 1989). Decollement thrust sheets are believed to have cut part of the Keweenawan Rift Basin into several adjacent sub-basins. These decollement thrust sheets may have been transported westward, leaving only the deepest rocks of the basin in place. Grenville foreland basin sediments were then deposited over the Keweenawan Rift event rocks. Post Grenvillian wrench faulting is believed to have destroyed much of the original thrust faulting in the region (Drahovzal, 1992; Steck, 1996).

Precambrian Unconformity and Basement Topography

The contact between the crystalline basement rocks of the Proterizoic and the sedimentary rocks of the Paleozoic is unconformable. After the Grenville Mountains were formed, they underwent heavy erosion for 300 million years during the Late Precambrian (see figure 7). The deep scouring away of the mountains exhumed their high-grade metamorphic roots. The erosion may have also removed the foreland basin

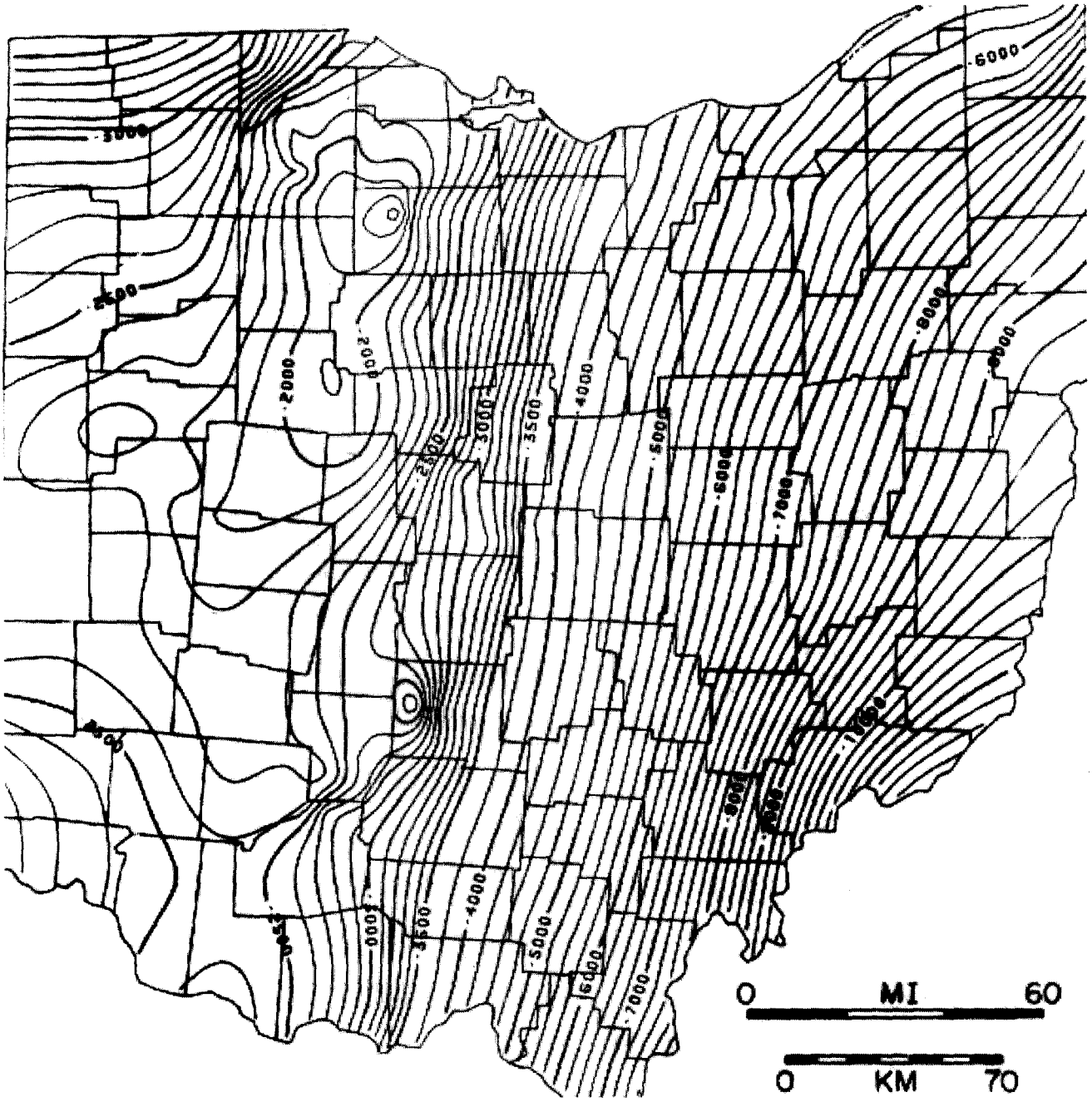

Figure 11. **Precambrian crystalline basement surface topography of Ohio. Modified from Lucius and Von Frese, 1988. Note the steep gradient of the drop-off of the basement in the center of the state. This demarcates the Grenville Front Tectonic Zone. Contour interval is 250 feet.**

sediments and the upper part of the ECRB. Extensive strike-slip and wrench faulting occurred close to the GFTZ during the Late Proterizoic. Some of these fault surfaces were reactivated during the Paleozoic (Drahovzal, 1992; Hansen, 1989). The faults in the study area are subparallel to the GFTZ, and it is believed that there was reactivation of faults beneath the Bellefontaine Outlier. The erosion scoured the surface of Late Proterizoic Ohio down to generally gently rolling terrain before sediment loading in the Paleozoic. Basement topography was mapped using available well data and magnetics (see figure 11). The top of the basement divided into three parts; the ECRB, the Grenville Province and the GRP. The Grenville Province lies to the east of the ECRB and the GFTZ. It dips from -2,500 to -5,000 feet in the north and to-12,000 feet elevation in the south. The GRP lies to the west of the ECRB. Its topography changes drastically from -7,500 to -25,000 feet elevation near the GFTZ and from -2,500 to 12,500 feet elevation near the Ohio-Indiana border. Normal faults having highly variable throws are also located close to the ECRB (Steck, 1997).

Paleozoic Sedimentary Stratigraphy

The Paleozoic is represented by Cambrian through Permian age sedimentary rocks, most of which are shales and dolomites (see figure 12). The structure of the basement, and reactivation of faults influenced deposition of Paleozoic sediments. Earliest Movement along the Logan-Hardin and Auglaize Faults are believed to occurred during the Cambrian or Early Ordovician. This fault movement is associated with regional extension tectonics. Reactivation of a lesser magnitude occurred along these faults during the Middle to Late Ordovician. The reactivation of these faults is believed to be responsible for the position of carbonate depositional platforms during the Ordovician (Wickstrom, 1990)(see figures 9 and 13). The Bellefontaine Outlier may have been topographically high during the Middle Devonian, because marine sediments that are present east of the area are missing on the Outlier. These units that are present in central

Ohio were deposited in shallow marine conditions. No Mesozoic or Tertiary age rocks are present in Ohio. Pleistocene glacial sediments cover the Paleozoic bedrock over most of Ohio and the Outlier. These sediments represent the Wisconsinan, Illinoian and pre-Illinoian Stages (Steck, 1997). Drainage patterns may have been influenced by the presence of faulting. The Teays River is believed to have carved out the rock around the Bellefontaine Outlier. Subsequent glaciation removed the surrounding rock, primarily limestone, but left the Outlier intact due to its cap of resistant shale.

Chapter 2: Bellefontaine Outlier

Introduction

The Bellefontaine Outlier is a steep highland in central Logan and northern Champaign Counties. West central Ohio is mostly flat glaciated plains, with exception to the scattered glacial moraines, most of which are at an elevation of 1000 feet above sea level. The relief and elevation of the Outlier is greater than that of the surrounding terrain. The average elevation of the Outlier (see figures 5 and 6) is 1400 feet above sea level, the highest point of which is located atop Campbell Hill (elevation of 1549 feet). The Bellefontaine Outlier is an isolated body of Devonian shales surrounded by Silurian carbonates. The nearest outcrop of Devonian rocks is located approximately 30 miles to the east in Delaware County (see figure 2). The bedrock of the Outlier and surrounding terrain is covered by glacial till. Campbell Hill is capped by 150 feet of glacial sediment (Hansen, 1996; Steck, 1997).

Stratigraphy

The stratigraphy of the Bellefontaine Outlier is comprised of rocks from the Proterizoic, Paleozoic and Cenozoic (see figure 12). The Proterizoic basement rocks of the Granite-Ryholite Province underlie much of the Outlier. The Middle Run Formation's

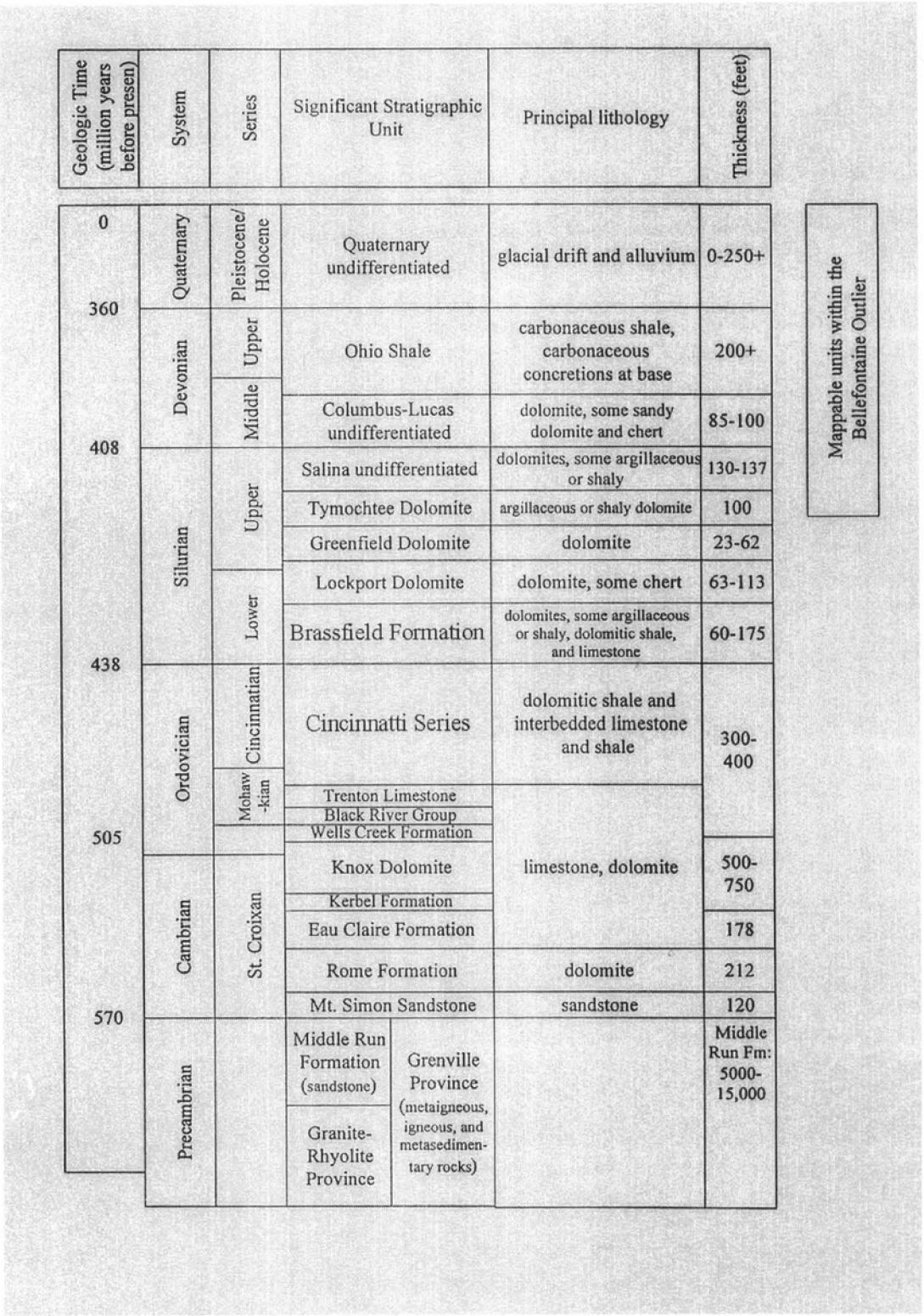

Geologic Time (million years before present)	System	Series	Significant Stratigraphic Unit		Principal lithology	Thickness (feet)
0	Quaternary	Pleistocene/ Holocene	Quaternary undifferentiated		glacial drift and alluvium	0-250+
360	Devonian	Upper	Ohio Shale		carbonaceous shale, carbonaceous concretions at base	200+
		Middle	Columbus-Lucas undifferentiated		dolomite, some sandy dolomite and chert	85-100
408	Silurian	Upper	Salina undifferentiated		dolomites, some argillaceous or shaly	130-137
			Tymochtee Dolomite		argillaceous or shaly dolomite	100
			Greenfield Dolomite		dolomite	23-62
		Lower	Lockport Dolomite		dolomite, some chert	63-113
			Brassfield Formation		dolomites, some argillaceous or shaly, dolomitic shale, and limestone	60-175
438	Ordovician	Cincinnatian	Cincinnatti Series		dolomitic shale and interbedded limestone and shale	300-400
		Mohawkian	Trenton Limestone		limestone, dolomite	
			Black River Group			
505			Wells Creek Formation			500-750
	Cambrian	St. Croixan	Knox Dolomite			
			Kerbel Formation			
			Eau Claire Formation			178
			Rome Formation		dolomite	212
			Mt. Simon Sandstone		sandstone	120
570	Precambrian		Middle Run Formation (sandstone)	Grenville Province (metaigneous, igneous, and metasedimentary rocks)		Middle Run Fm: 5000-15,000
			Granite-Rhyolite Province			

Mappable units within the Bellefontaine Outlier

Figure 12. **Generalized stratigraphic column of rocks in the Bellefontaine OutlierSurvey Area. Modified from Steck, 1997.**

clastics and volcanics over lie the Granite-Ryholite Province. Grenville Province metaigneous, igneous and metasedamentary rocks are present in the northeastern corner of the study area. The Paleozoic section in Ohio is characterized by transgressive and regressive events recorded in the sedimentary rocks of the Cambrian, Ordovician, Silurian, and the Devonian. Cambrian sediments are primarily limestones, dolomites and sandstones. Ordovician sediments are primarily dolomitic shales interbedded with limestone and shale. Argilaceous to shaley dolomites, limestones and dolomitic shales make up the stratigraphy for the Silurian. The Devonian consists of dolomites and carbonaceous shales. The Devonian bedrock is capped by a thick cover of Quaternary glacial till (Hansen,1996; Steck, 1997).

Structure of the Bellefontaine Outlier

The Bellefontaine Outlier is a highland of Devonian shale surrounded by older Silurian strata. The Outlier was originally considered to be an erosional remnant that escaped erosion due to random preglacial drainage patterns. Recent evidence from COCORP OH-1 seismic line and other workers (Steck et. al.,1997; Noltimier et. al., 1998) have interpreted the Outlier lying above a reverse basement graben. The Bellefontaine Outlier is situated over thrust faults of the Grenville Front Tectonic Zone. High angle reverse faults are thought to surround the crustal block containing the Bellefontaine Outlier. This would allow the block to drop and be situated adjacent to rocks of an older age. The COCORP OH-1 revealed near vertical basement depth faults that cut through the Paleozoic rocks and to the near surface (Pratt et al., 1989; Weaver, 1994; Steck, 1997). These faults may be prone to reactivation under induced stress. The Logan-Hardin, Auglaize, Bowling Green and Union Faults are believed to have been exposed to such reactivation (see figures 13 and 14). The Bellefontaine Outlier is on the northeastern edge of the Cincinatti Arch and south of the Findlay Arch. It is centered between the Appalachian, Illinois and Michigan Basins, and is located within the Fort

Wayne Rift (Steck, 1996; Wickstrom, 1990).

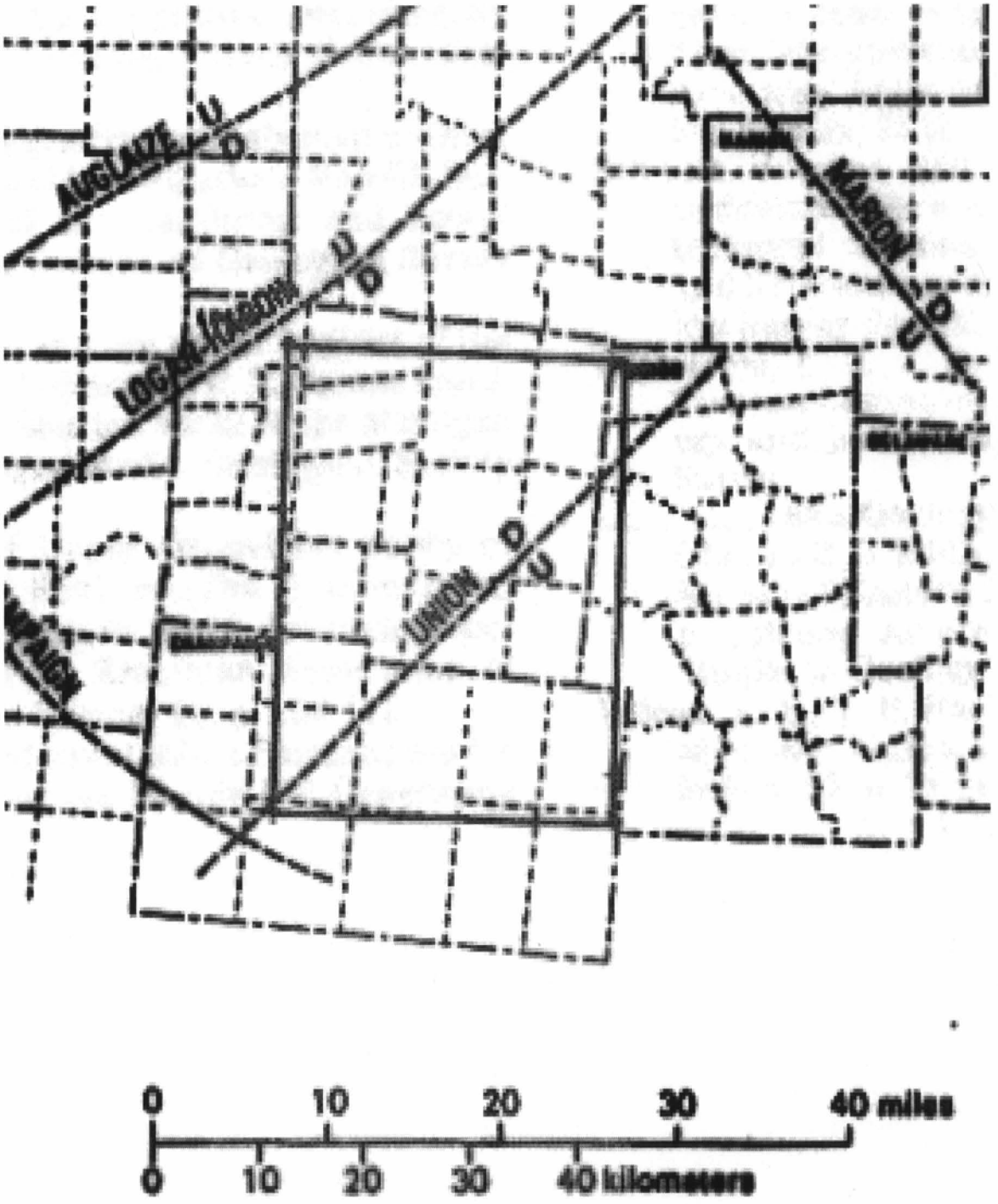

Figure 13. **Map of down to basement faults in west central Ohio. These faults are thought to represent northeast-trending blocks of graben and reverse graben structures. Modified from Wickstrom, 1990.**

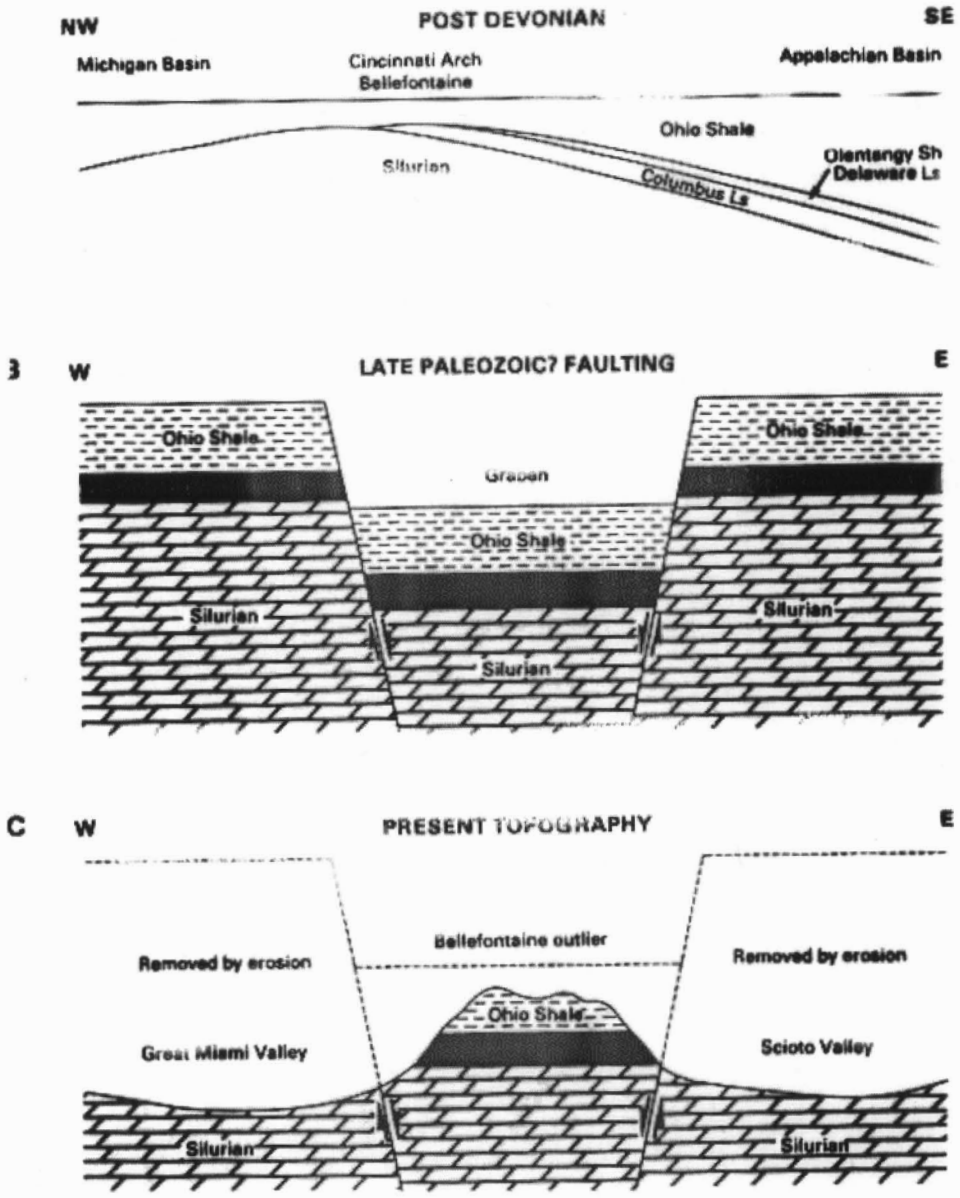

Figure 14. **Development of the Bellefontaine Outlier during the Paleozoic. Note the Paleozoic faulting that resulted in the graben structure. It is believed that reactivation of deep basement faults resulted in fracturing of Paleozoic rocks. Modified from Steck et.al, 1997.**

Chapter 3: Magnetic Profiles

Introduction

The main objective of this study is to examine the magnetic anomalies produced by faulting within the deep basement. Ferromagnetic minerals in igneous and metamorphic rock affect the earth's normal geomagnetic field. For this reason crystalline basement rocks and inconsistencies within them are the primary source of magnetic anomalies. Sedimentary rocks that cover these basement rocks are invisible to magnetic study (see table 1). Therefore, for my study of the Bellefontaine Outlier, only the Precambrian crystalline basement will be considered. All field data was collected by Weaver (1994), who used a G-856 Memory Mag Proton Precision magnetometer for the magnetic survey. A total of 550 field stations were set up within the study area, allowing for a more precise examination of the Bellefontaine Outlier (see figure 15). Weaver's field data is used in my paper to construct the maps and profiles. The profiles in my paper were constructed coincident to Steck (1997) using the 300 gamma-filtered geomagnetic residual map modified from Weaver. The purpose is to compare the fault placement and throw between gravity and magnetic anomaly interpretation.

Methods

As in Steck's thesis some basic assumptions were made concerning the structure and lithology of the Bellefontaine Outlier. All faults were considered to be vertical or near vertical to simplify the calculation of fault throw using magnetics. The Paleozoic strata covering the Outlier is essentially ignored as its magnetic signature is small compared to that of the underlying Precambrian rocks. The magnetization of the rocks **J** was initially considered to be 10^{-1}oe., which is the magnetization of basalt (the agreed upon lithology for basement underneath the Outlier, as per the1997 GSA). However the resultant fault throws were very small compared to Steck's. Consequently, the value of **J**

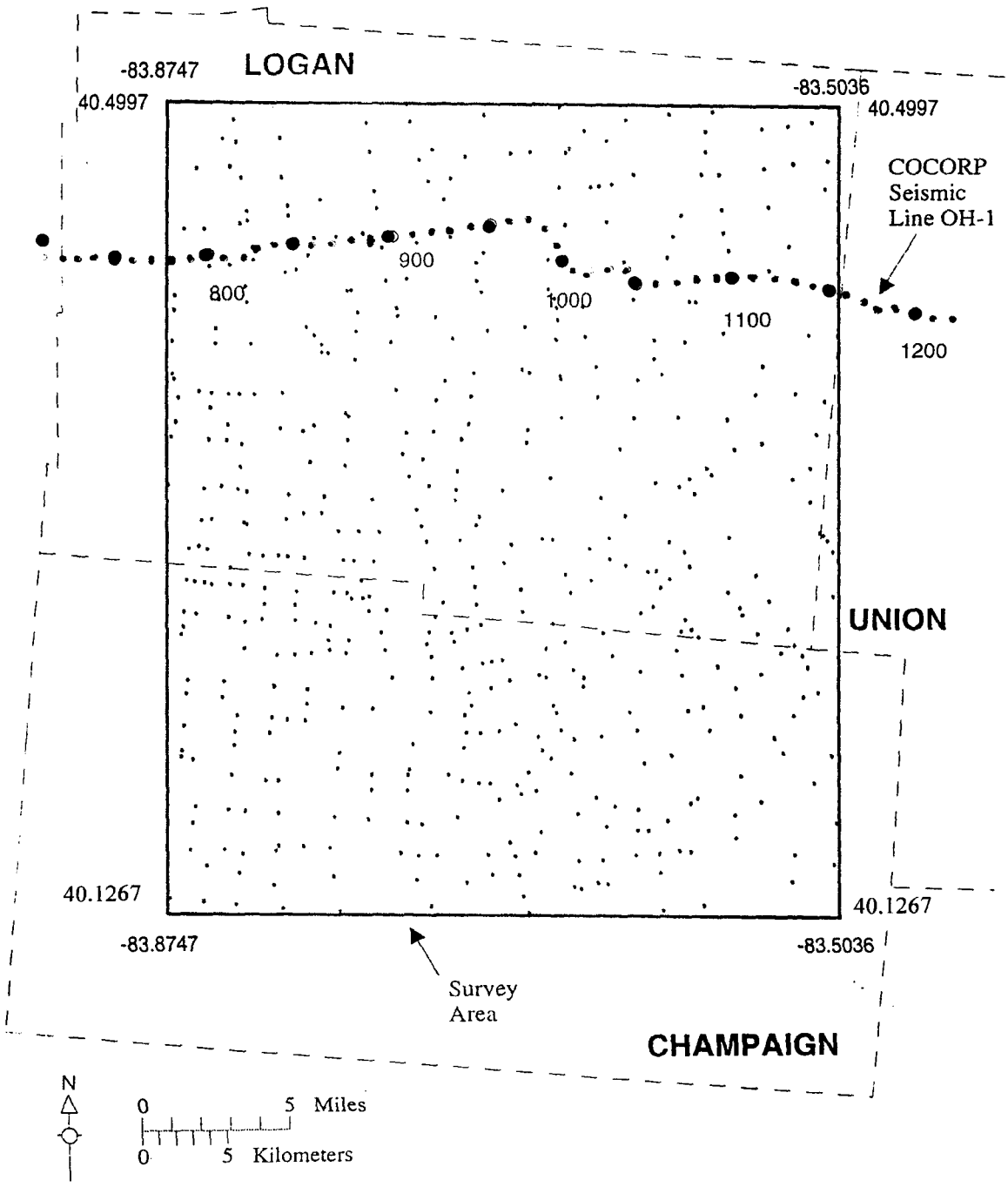

Figure 15. Map of survey area showing relative positions of field stations for gravity and magnetics. From Steck, 1996.

was decreased to adjust the fault throws to those of Steck's. The magnetization of the rocks underneath the Outlier is taken to be within the adjusted values between $10^{-1.8}$ and $10^{-2.9}$ oe. It seems likely that this variation in the assumed magnetization could be due to changes in igneous lithology within the study area. There is no evidence to support or disclaim this but my assumed values for **J** are quite reasonable.

The magnetic profiles were examined for inflection points where the curvature of the peaks and valleys of the profile changed. The point on the profile where the curvature changed is considered to be the locality a fault. It was by this method that the faults within the study area were identified. The Precambrian crystalline basement structure map produced by Wickstrom (1990) was also used to help calculate the throw of the faults by providing the average depth to basement across the faults.

Table 1

Magnetization values for rocks in the study area (Weaver, 1994).

Rock type	**Magnetization of the rock (oe)** **Magnetization is expresed in cgs units.** **1 gamma = 10^{-5} oersteads**
Limestone	10^{-6}
Lithic sediments	10^{-6} to 10^{-5}
Shale	10^{-5} to 10^{-4}
Rhyolite	10^{-4} to 10^{-3}
Basalt	10^{-1} to 10^{-2}
Ferromagnetic minerals	$>10^{-1}$

Figure 16. Total field geomagnetic map with 300 gamma filter. Profile traverses are provided. Modified from Weaver 1994.

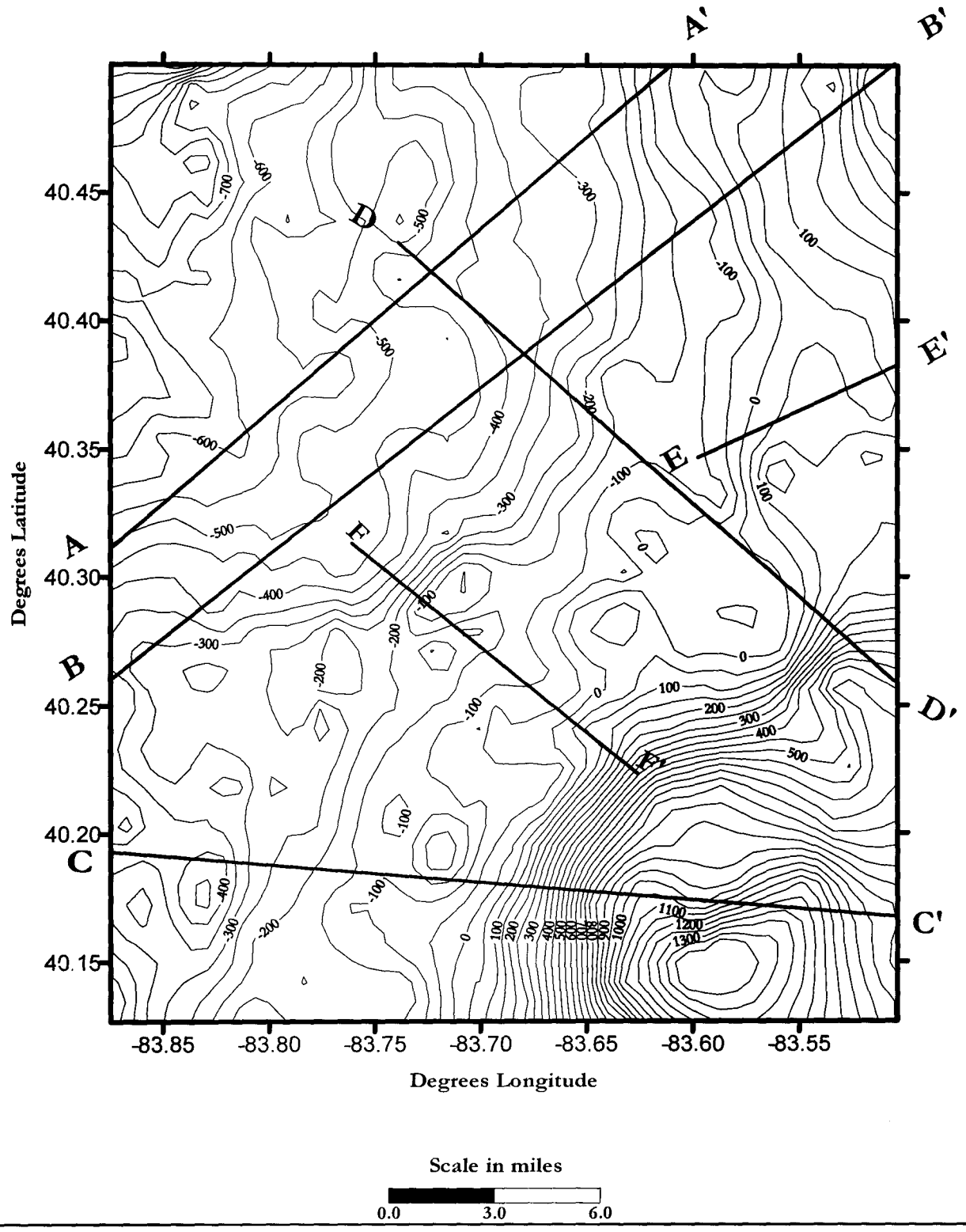

Sample Calculation/Calculations

Derivation of fault throw formula.

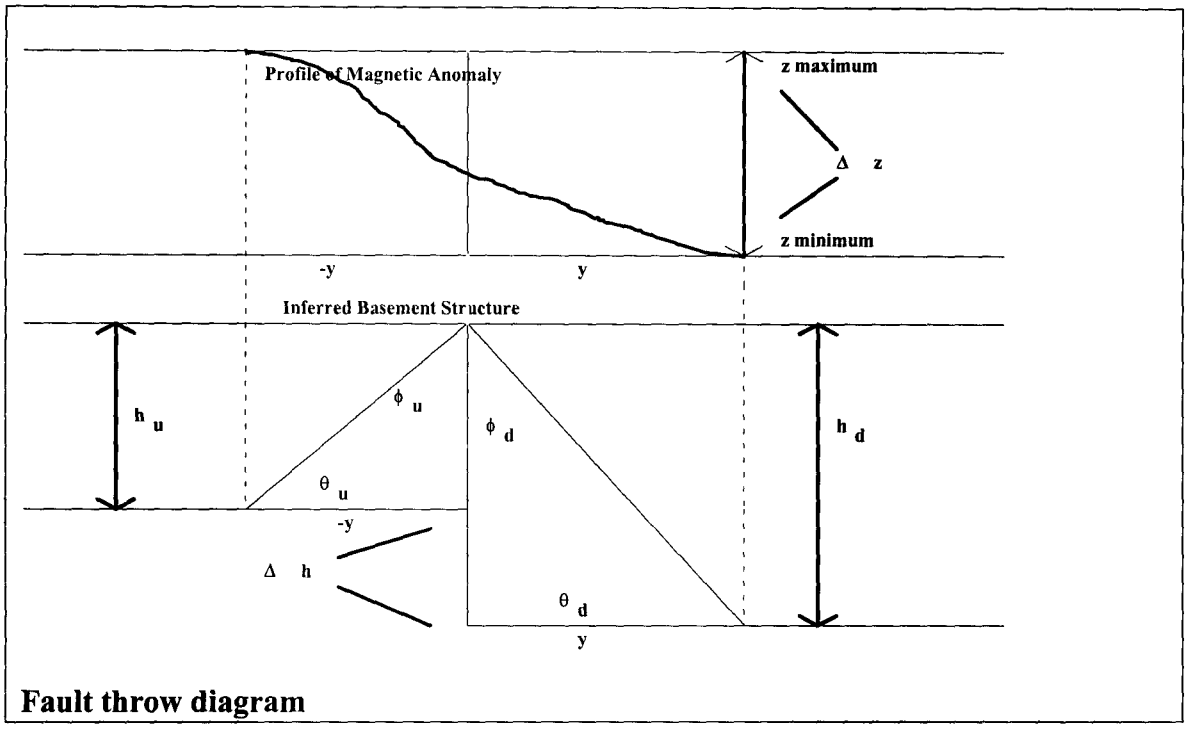

Fault throw diagram

Δz =Amplitude of magnetic anomaly (z_{max}-z_{min}).

y = Half-length of magnetic anomaly. Estimated from profiles by taking 1/2 horizontal distance between z_{max} and z_{min}. This distance must then be converted from degrees to kilometers. The conversion factor varies between profiles, but it follows the following formula;

1/2 * (Angular distance in degrees between z_{max} and z_{min}) * (Total angular distance of profile in kilometers/0.32°).

Δh = Fault throw (h_d-h_u).

ϕ_υ,ϕ_d = Angle between fault plane to top of up/down thrown block distance y from fault.

θ_u, θ_d = Angular distance along top of up/down blocks in radians.

$\Delta\theta = \theta_d - \theta_\upsilon$

Of greatest interest in analyzing magnetic anomaly profiles are curves of gradient change.

The magnetic effects of faulting and lithologic changes in the basement rocks are reflected by changes in the gradient of the magnetic anomaly profiles. Assuming a near vertical fault plane, one may calculate the amplitude of the magnetic anomaly using the following expression;

$\Delta z = 2J\Delta\theta$ (Noltimier, 1997). **J** = Magnetization of the rocks at the fault. **J** is measured in gammas, but is converted to oersteads for the calculation. 1 gamma = 10^{-5} oersteads.

The expression $\Delta z = 2J\Delta\theta$ can be expanded by stating $\Delta\theta = \theta_d - \theta_u$.

From figure_ the following relationships apply;

$\tan\phi_u = (y/h_u)$ and rearranging $\phi_u = \tan^{-1}(y/h_u)$

$\tan\phi_d = (y/h_d)$ and rearranging $\phi_d = \tan^{-1}(y/h_d)$

Convert ϕ degrees to θ radians. We don't need to calculate this as we are just stating how ϕ is related to θ.

$\phi_u * 0.01745 = \theta_u$

$\phi_d * 0.01745 = \theta_d$

Given the equation $\Delta z = 2J\Delta\theta$, where $\Delta\theta = \theta_u - \theta_d$. $\Delta\theta$ is a function of the throw Δh. The function of Δh comes from the Taylor Series Expansion for $\tan^{-1}x$. **Let (y/h) = x.**

$\tan^{-1}x = x - x^3/3 + x^5/5 - x^7/7 + \ldots$ $x^2 < 1$ The first term is considered only because increasing powers of x are increasingly small. These can be largely ignored because their net effect upon the calculation is negligible. The angle ϕ is taken to be very shallow, such that the fault and the hypotenuse are nearly congruent. We are able to state the approximation;

$\tan^{-1}x = x$. And therefore the following approximations are true;

$\theta_u = x_u = (y/h_u)$

$\theta_d = x_d = (y/h_d)$

$\Delta\theta = \theta_u - \theta_d = (y/h_u - y/h_d)$

Factoring y the expression becomes

$\Delta\theta = y(1/h_d - 1/h_u)$.

Using algebraic manipulation,

$\Delta\theta = y[(h_u - h_d)/h_d h_u]$.

Factoring the denominator from the expression $\Delta\theta = y[(h_u - h_d)/h_d h_u]$, we get;

$hdhu = (h + \Delta h/2)(h - \Delta h/2)$.

$= (\underline{h}^2 - \Delta h^2/4)$

Which gives us;

$\Delta\theta = y[(h_u - h_d)/(\underline{h}^2 - \Delta h^2/4)]$.

The term $\underline{h}$ is the mean depth to the top of the Precambrian crystalline basement. This value is found on ***Wickstrom's Precambrian crystalline basement structure map***, figure 17. We take this at the midpoint of the fault. Δh is the fault throw $(h_d - h_u)$.

The expression $(\Delta h^2/4)$ is disregarded because it is smaller than $\underline{h}^2$. That is, any contribution by $(\Delta h^2/4)$ is smaller than that of $\underline{h}^2$. Considering only $\underline{h}^2$ in the denominator, our expression for $\Delta\theta$ becomes;

$\Delta\theta = y[(h_u - h_d)/h_d h_u] = y(\Delta h/\underline{h}^2)$ (Noltimier, 1997).

Substituting $\Delta\theta = y(\Delta h/\underline{h}^2)$ into the equation for the amplitude of a magnetic anomaly, the new equation is;

$\underline{\Delta z = 2Jy(\Delta h^2/h^2).}$

This equation is then arithmetically rearranged to solve for the throw of faults in the basement using magnetic anomaly interpolation.

The throw of a fault in the basement rock is defined by the equation; $\Delta h = [(\Delta z \underline{h}^2)/(2Jy)]$.

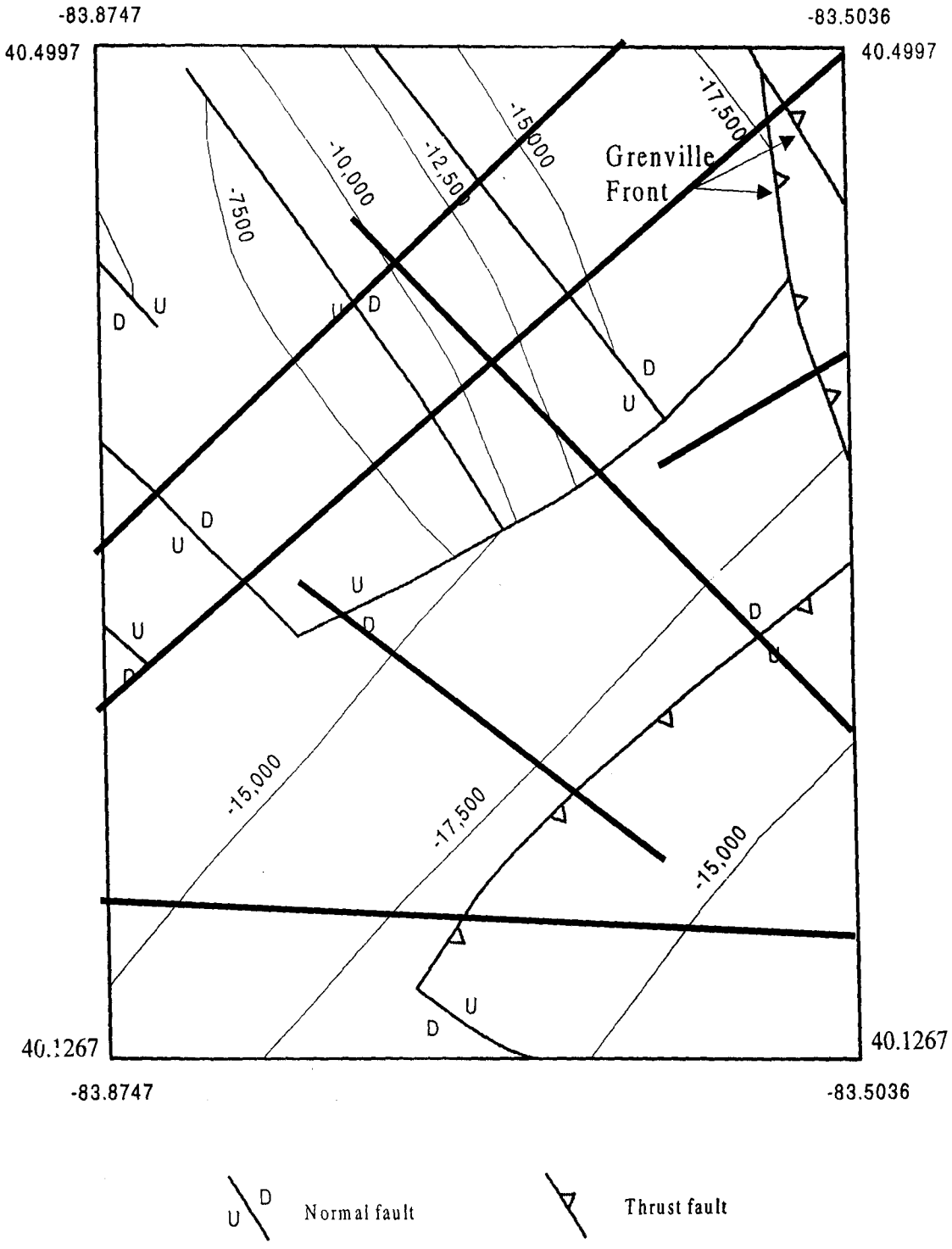

Figure 17. **Wickstrom's structure contour map of the Precambrian crystalline basement surface in the Bellefontaine Outlier Study Area. Contour interval is 2500 ft. Modified from Steck, 1997.**

Table 2

Values of magnetic amplitude, anomaly length, conversion factors, magnetization, and fault throws for the magnetic anomaly profiles.

Fault #	Δz Amplitude of Magnetic Anomaly in gammas $1\gamma = 10^{-5}$oe	2y Anomaly Length in Degrees	Conversion Factor for Length (deg°/km)	y Anomaly Half Length in km	h Mean Basement Depth Across Fault (km)	h^2 (km^2)	J Magnetization of the rock in (oe) (log 10 oe)	Δh Throw of the Fault (km)
A-1	140	0.07	27.35/0.32	2.99	2.287	5.23	-1.8	0.08
A-2	525	0.19	27.35/0.32	8.12	3.429	11.76	-1.9	0.38
B-1	230	0.12	55.10/0.44	7.52	2.287	5.23	-1.8	0.13
B-2	320	0.12	55.10/0.44	7.51	4.19	17.56	-2	0.37
B-3	250	0.12	55.10/0.44	7.51	4.88	23.78	-2	0.87
C-1	1200	0.1	41.84/0.37	5.65	4.95	24.53	-2	2.6
D-1	440	0.15	41.83/0.28	11.2	3.43	11.76	-2.2	0.37
D-2	600	0.08	41.83/0.28	5.98	4.95	24.53	-2.2	1.95
E-1	170	0.06	11.49/0.10	3.45	4.95	24.53	-2.1	0.76
F-1	400	0.05	25.74/0.21	3.06	3.43	11.76	-2.1	0.97
F-2	1000	0.14	25.74/0.21	8.58	4.95	11.76	-2.2	2.27

Magnetic Anomaly Profile Interpretations

Profile A

Two faults were interpreted from the magnetic profile of A (see figure18). Fault A-1 is located on the western side of the profile and its amplitude is approximately 140 gammas. The southwestern side of fault A-1 is interpreted to be upthrown from the magnetics, the northeastern side down thrown. The throw of fault A-1 is calculated to be 0.08 km. Fault A-1 is not as pronounced as fault A-2 to the east. This may be due to the oblique angle at which the profile was constructed to the apparent graben structure trending NE-SW on the magnetic map (see figures 16, 24 and 25). Fault A-2 produces a larger magnetic anomaly, of the magnitude of 525 gammas. The southwestern side of the fault is interpreted to by down and the northeastern side is up. The throw of Fault A-2 is approximated to be between 0.30 and 0.38 km. To the east the magnetic profile steadily climbs from -600 to 0 gammas due to the magnetic influence of the Grenvile Front Tectonic Zone.

Profile B

Profile B was interpreted to have three faults form the magnetics (see figure 19). Steck (1994) interpreted from the gravity to state that there three faults present. Interpretation of the magnetics agrees that three faults along Profile B exist. The magnetic signature of profile B climbs to nearly 400 gammas at the northwestern boundary of profile B. This is due to the magnetic effect of the edge of the Grenville Front Tectonic Zone. Fault B-1 is located approximately 0.07 angular degrees along the profile. The magnitude of the magnetic anomaly produced by B-1 is 230 gammas. The calculated fault throw of B-1 is 0.13 km. The southwestern side of fault B-1 is interpreted to be up, the northeastern side down. Fault B-2 is located approximately 0.26 angular degrees along the profile. The amplitude of the magnetic anomaly produced by B-2 is 320 gammas. The calculated fault throw for B-2 is 0.37 km. The southwestern side of

Figure 18. Profile A-A' from gravity and magnetic anomaly maps of the Bellefontaine Outlier.

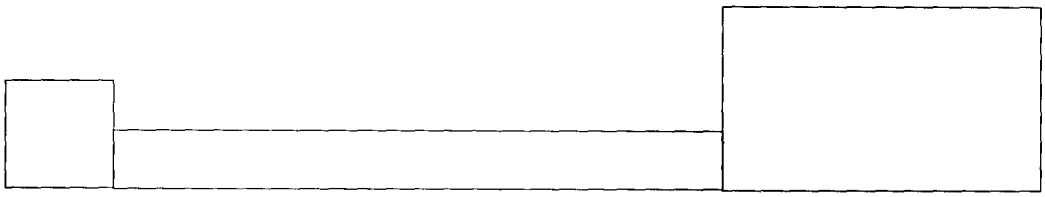

Inferred basement structure of profile A

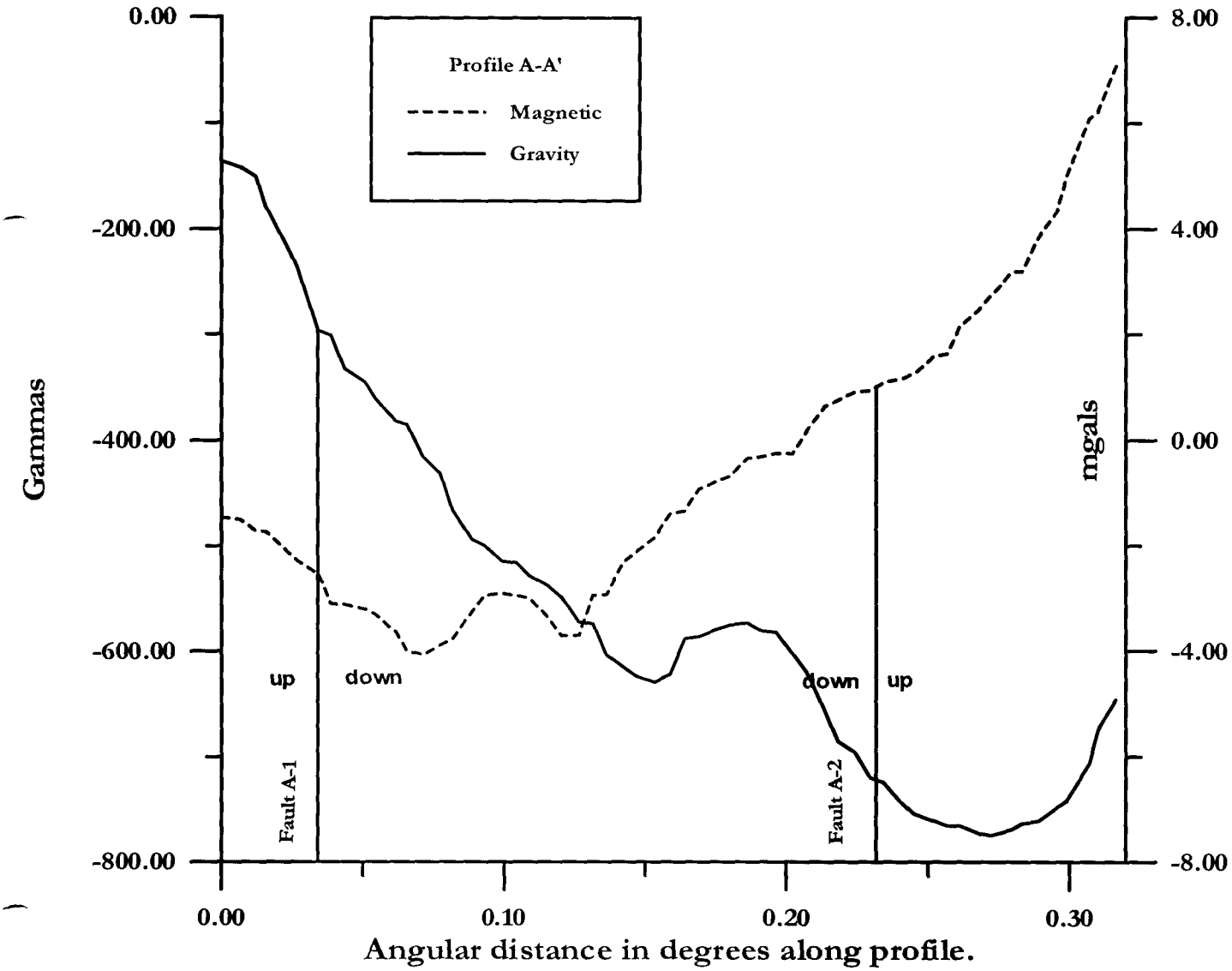

Figure 19. Profile B-B' from CBRA and total filtered magnetic anomaly maps of the Bellefontaine Outlier.

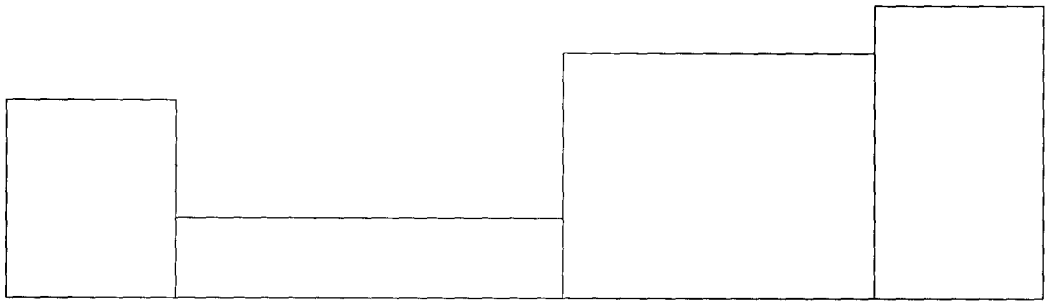

Inferred basement structure from profile B.

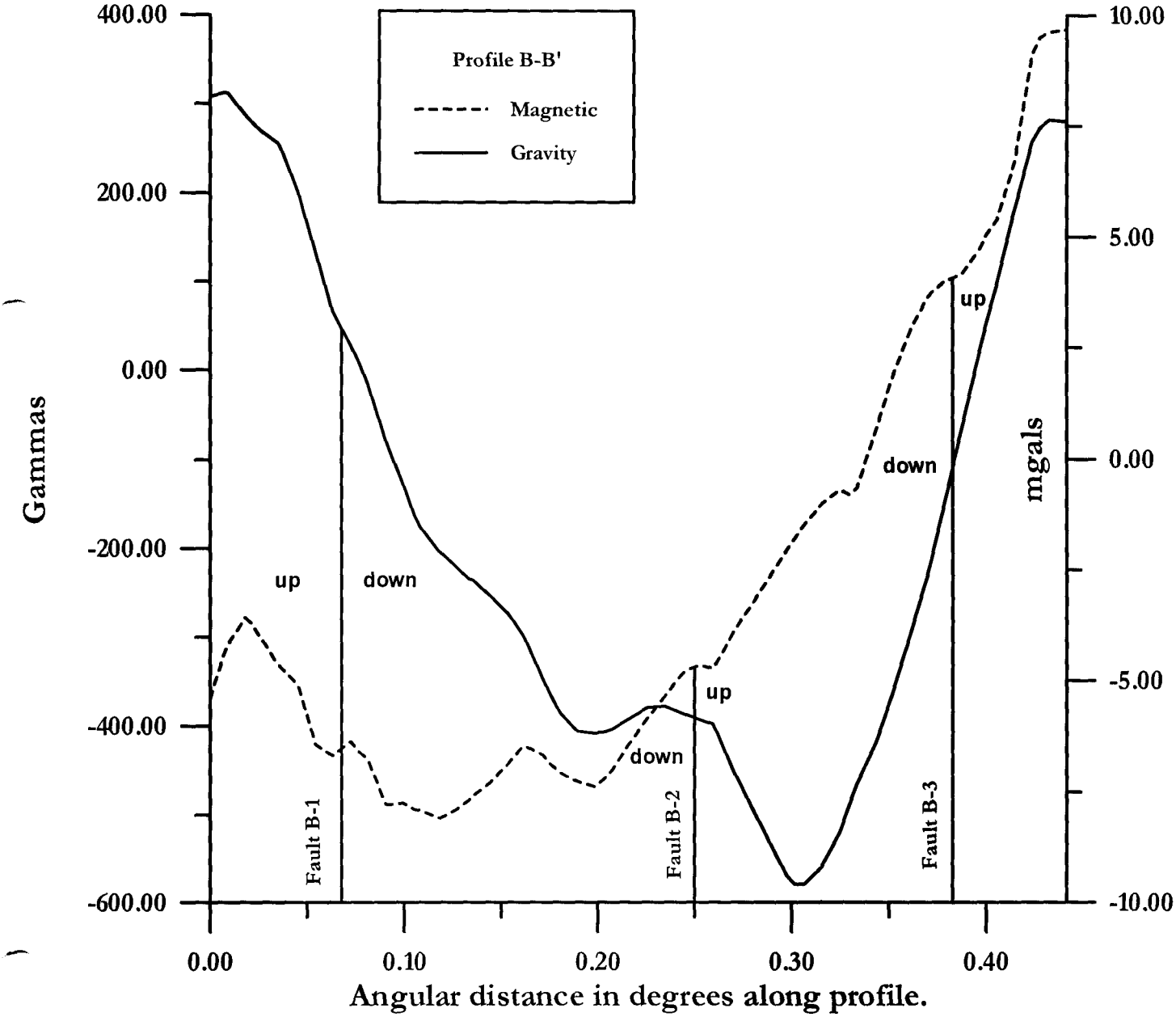

Figure 20. Profile C-C' from CBRA and total filtered magnetic anomaly maps of the Bellefontaine Outlier.

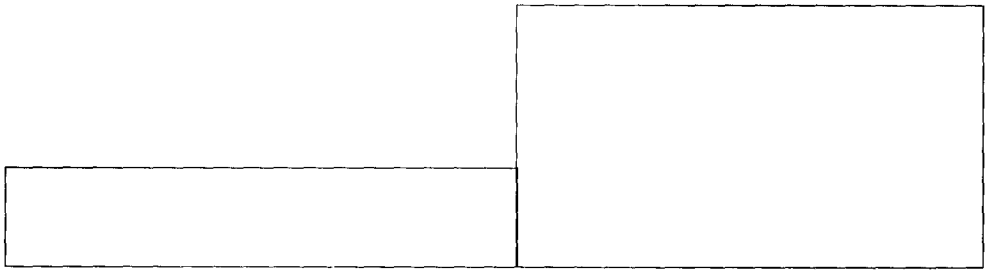

Inferred basement structure of profile C

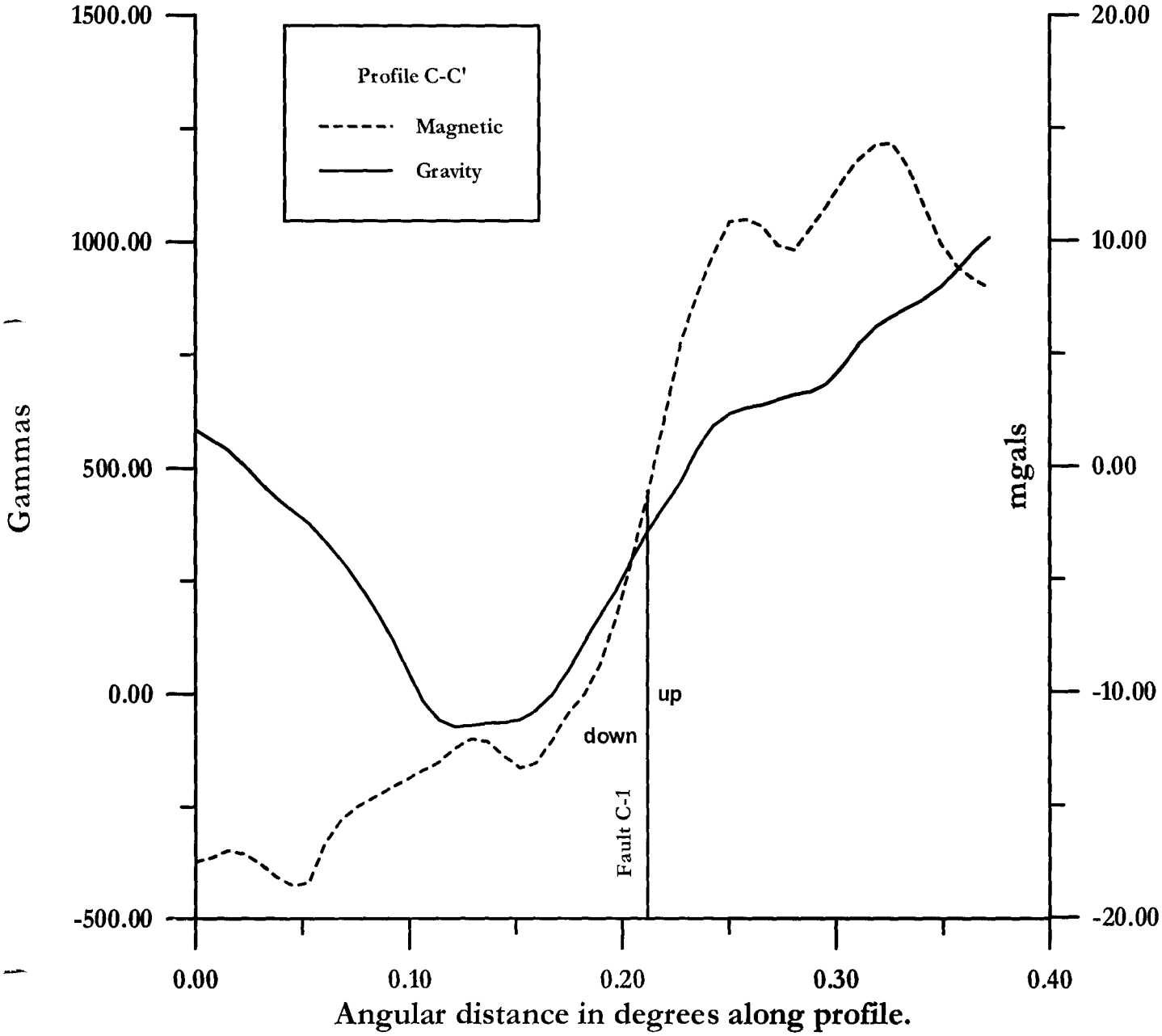

Figure 21. Profile D-D' from CBRA and total filtered magnetic anomaly maps of the Bellefontaine Outier.

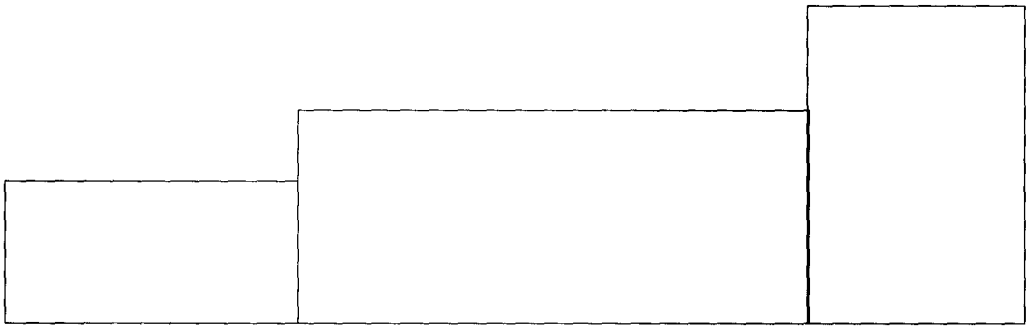

Inferred basement structure for profile D.

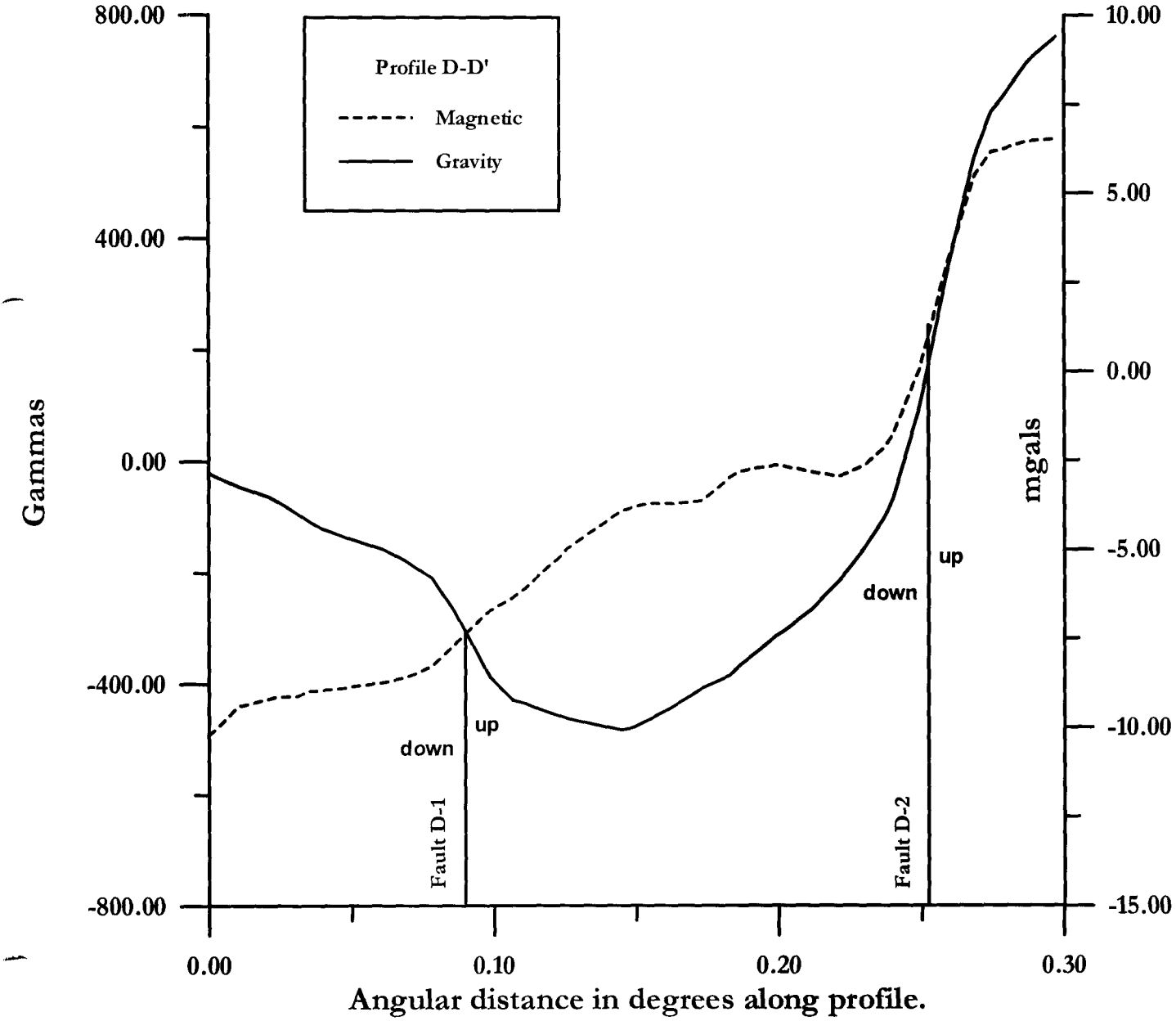

Figure 22. Profile E-E' from CBRA and Total Filtered Magnetic Anomaly Maps of the Bellefontaine Outlier.

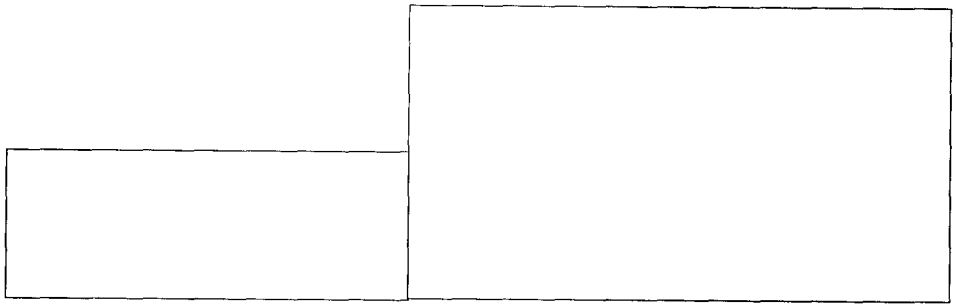

Inferred basement structure for profile E.

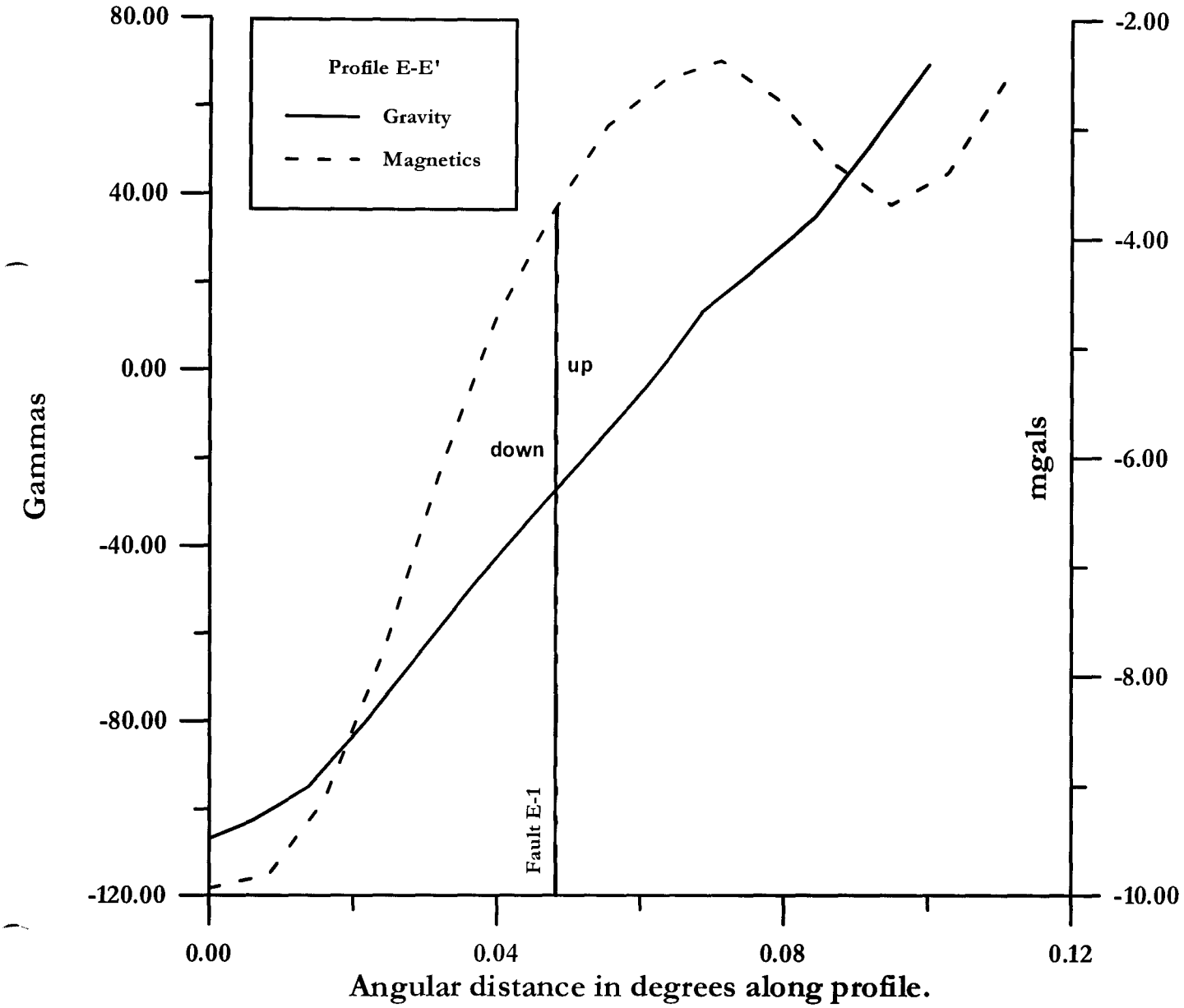

Figure 23. Profile F-F' from CBRA and total filtered magnetic anomaly maps of the Bellefontaine Outlier.

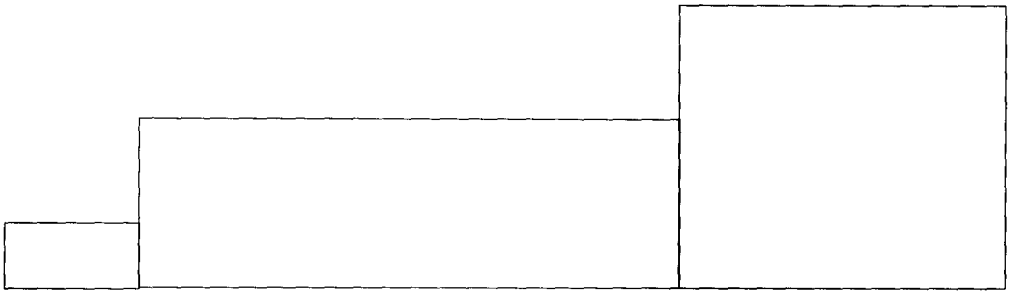

Inferred basement structure for profile F.

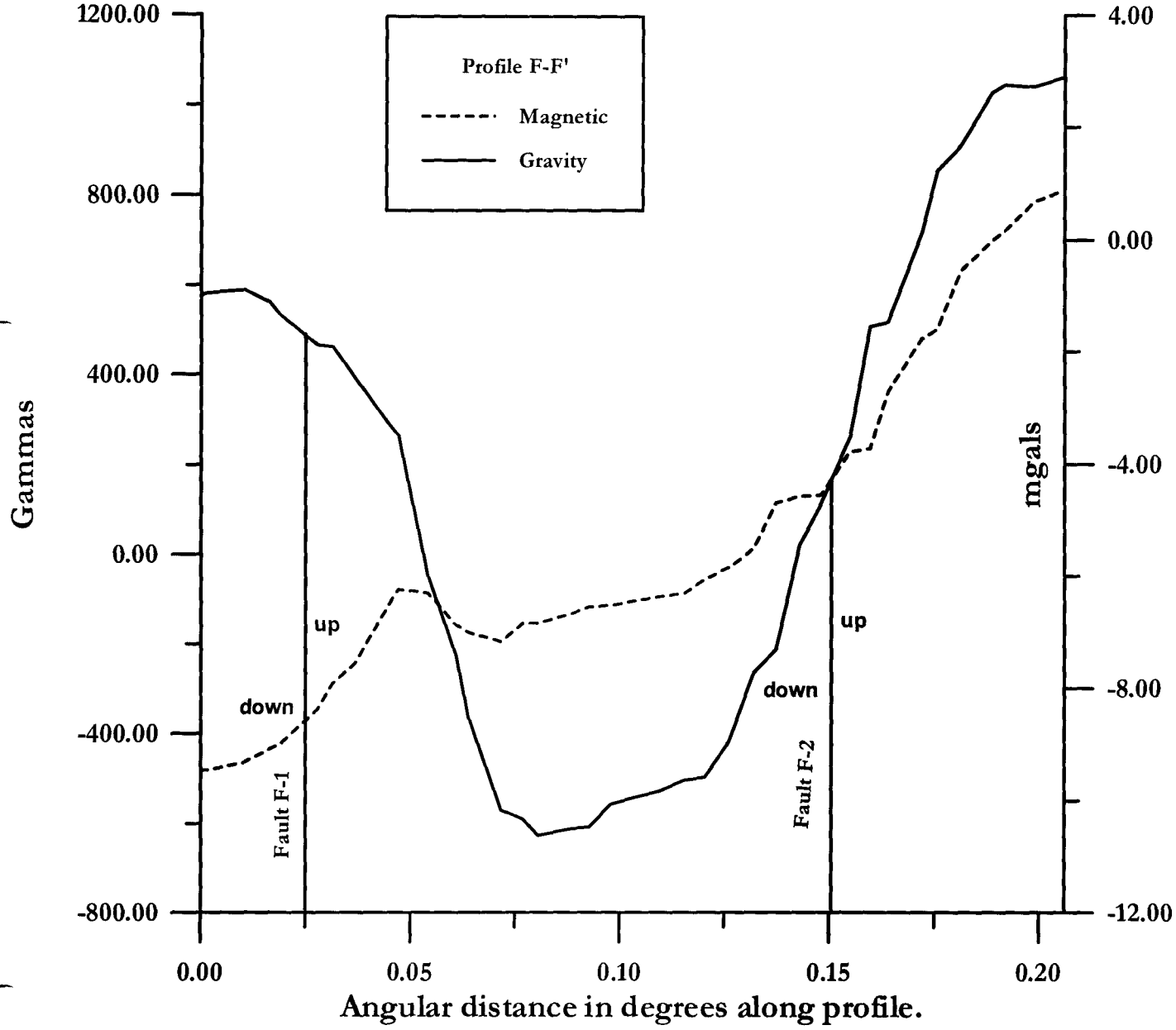

fault B-2 is interpreted to be down, the northeastern side is up. Fault B-3 is located immediately northeast of fault B-2 at 0.39 degrees angular degrees along profile B. The anomaly produced by this fault is easily recognizable from the change in concavity in its profile. The amplitude of fault B-3 is approximately 250 gammas. The calculated throw of fault B-3 is 0.87 km. The southwestern side of the fault is interpreted to be downthrown in respect to the northeastern upthrown side.

Profile C

From the magnetic anomaly data profile C indicates the presence of a fault and a volcanic plug or possibly an ore body (see figure 20). The profile was constructed across a very magnetic body, and the determination of the presence of faulting was difficult. It is believed that the presence of a fault on the border of the magnetic body accentuates the magnetic anomaly it produces. Also referring to the regional magnetic map(see figures 24 and 25), the western shoulder of the magnetic body is quite steep, quite possibly due to faulting around the perimeter of the body (Noltimier, personal communication). Steck (1997) interpreted there to be to faults within profile C using gravity anomaly interpretation. However, using magnetics, I found that there was only one recognizable fault. The magnetic anomaly profile of C is dominated by the anomaly of the magnetic body, however it is believed that the anomaly generated from faulting did accentuate the amplitude of the magnetic body, therefore it was calculated. Fault C-1(?) is located approximately 0.20 angular degrees along the profile. The amplitude of this anomaly is large due to the localized effects of the volcanic plug or ore body. The amplitude of the magnetic anomaly over fault C-1 is 1200 gammas. The western side of fault C-1(?) appears to be downthrown and the eastern side appears to be upthrown. The throw of fault C-1(?) was calculated to be 2.60 km. This is a large throw compared to Steck, 1997. Other faulting along the profile was not recognizable from the magnetics and small variations were ignored. This may be do as well from the magnetic volcanic or ore body. Gravity anomaly interpretation by Steck (1997) was able to identify one other fault. I

however, was unable to do so.

Profile D

Profile D has at least one fault and possibly one other bordering a volcanic plug or ore bodies (see figure 21). The magnetic gradient increases from -500 gammas in the northwest to 560 gammas in the southeast. This rapid gradient change is due to the fact that the profile lies over a part of the volcanic plug, possibly a failed pipe or peroditite pod, in the southeastern corner of the study area (see figures 16, 24 and 25). Fault D-1 is located on profile D 0.08 angular degrees. The anomaly is gently curving and broad, yet has an amplitude of 440 gammas. The northwestern side of the fault is believed to the downthrown side and the southeastern side is upthrown. The throw of fault D-1 is calculated to be 0.37 km. The anomaly identified as fault D-2(?) may be influenced by the magnetic anomaly produced by the volcanic plug or ore body in the southeaster corner of the study area. Fault D-2(?) can be inferred by the magnetics, for it can be argued that the magnetic anomaly of the fault accentuates the shape of the anomaly produced by the magnetic body. It may also be valid to state that faulting around the volcanic plug or an ore body seems likely. For these reasons the approximate placement and throw of fault D-2(?) was determined. Fault D-2(?) is located approximately 0.25 angular degrees along profile (see figure 21). The anomaly is quite pronounced rising from 0.00 gammas to 600 gammas. The northwestern side of the fault is interpreted to be downthrown and the southeastern side is upthrown. The throw of fault D-2 is calculated to be 1.95 km. The magnitude of the magnetic anomaly produced by the volcanic plug is approximately 560 gammas. From the magnetic map (see figure of magnetic map) it appears that this body may be an extension of the body in the southeastern corner of the study area.

Profile E

Profile E contains one fault not reflected in the gravity anomaly investigation by Steck, 1996 (see figure 22). Fault E-1 is located 0.05 angular degrees along profile E. The southwestern side of the fault is interpreted to be downthrown and the northeastern side is upthrown. The amplitude of the magnetic anomaly is approximately 170 gammas. The calculated fault throw is 0.76 km.

Profile F

Profile F contains one fault and possibly another bordering a volcanic plug. Fault F-1 wasn't identifiable in the gravity anomaly profile by Steck, but it registered well with magnetics (see figure 23). Fault F-1 is located 0.025 angular degrees from the northwestern side of profile F. The amplitude of the anomaly produced by fault F-1 is approximately 400 gammas. The northwestern side of the fault is interpreted to be downthrown and the southeastern side is upthrown. The calculated fault throw of fault F-1 is 0.97 km. The presence of fault F-2(?) may be inferred by the magnetics, for it can be argued that the magnetic anomaly of the fault accentuates the shape of the anomaly produced by a magnetic body. It may also be valid to state that faulting around a volcanic plug or an ore body occurs quite frequently. For these reasons the approximate placement and throw of fault F-2(?) was determined. (see figures 16, 24 and 25). Fault F-2(?) is located 0.150 angular degrees along profile F. The anomaly produced by fault F-2(?) is characterized by a large amplitude and broad horizontal displacement (see figure 23). The large amplitude of the anomaly is also undoubtedly due to the presence of the magnetic volcanic plug or ore body over which the profile is constructed. The amplitude of the anomaly over fault F-2 is 1000 gammas. The fault throw is calculated to be 2.27 km.

Figure 24. Total field geomagnetic map with 300 gamma filter. Location of faults are provided. Solid lines are definite fault placement, dotted lines are questionable. Contour interval is 50 gammas.

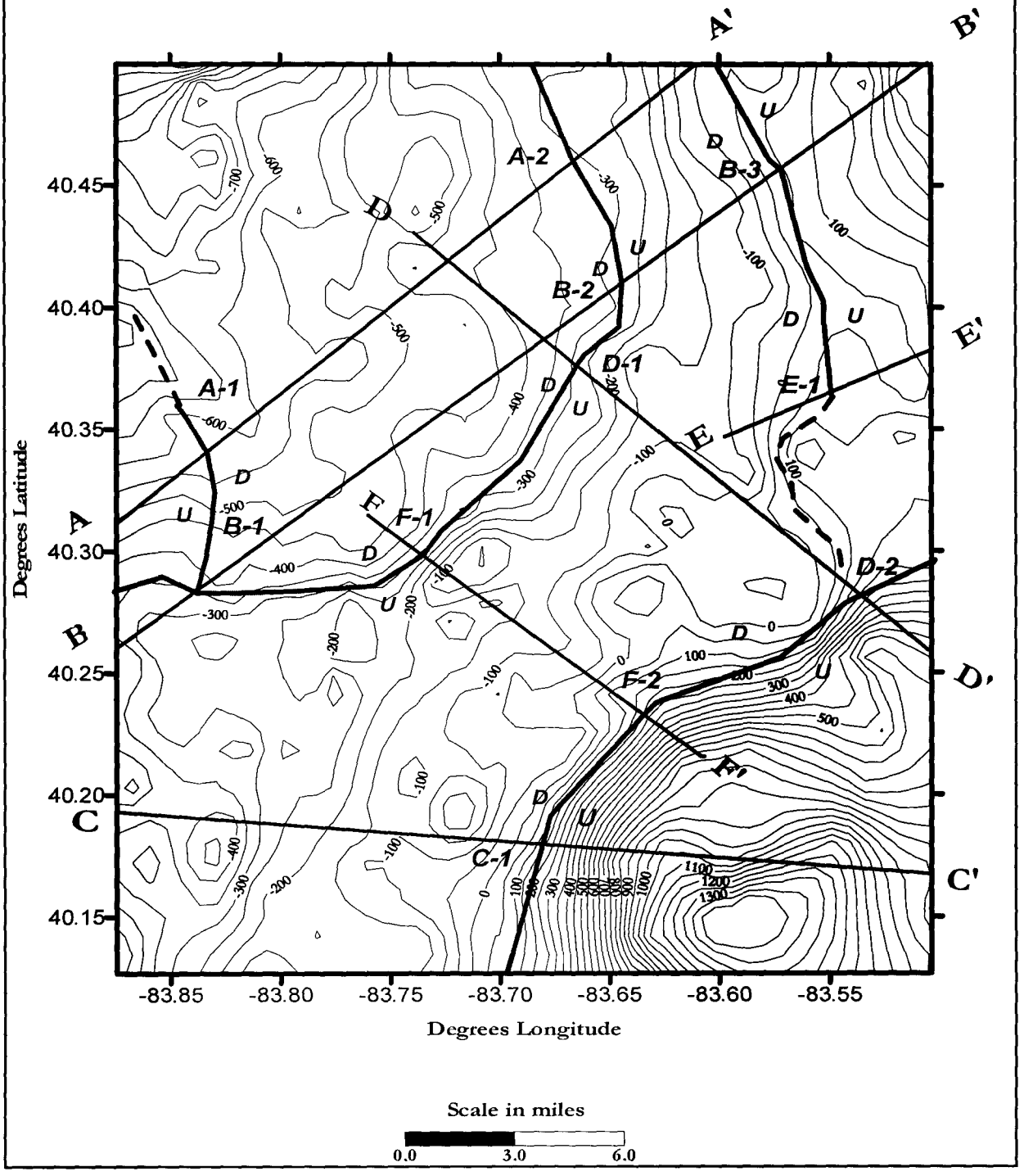

Figure 25. 3-D 300 gamma filered total residual anomaly map with fault placement. Notice the gradient on the large amplitude anomaly in the right corner of the figure.

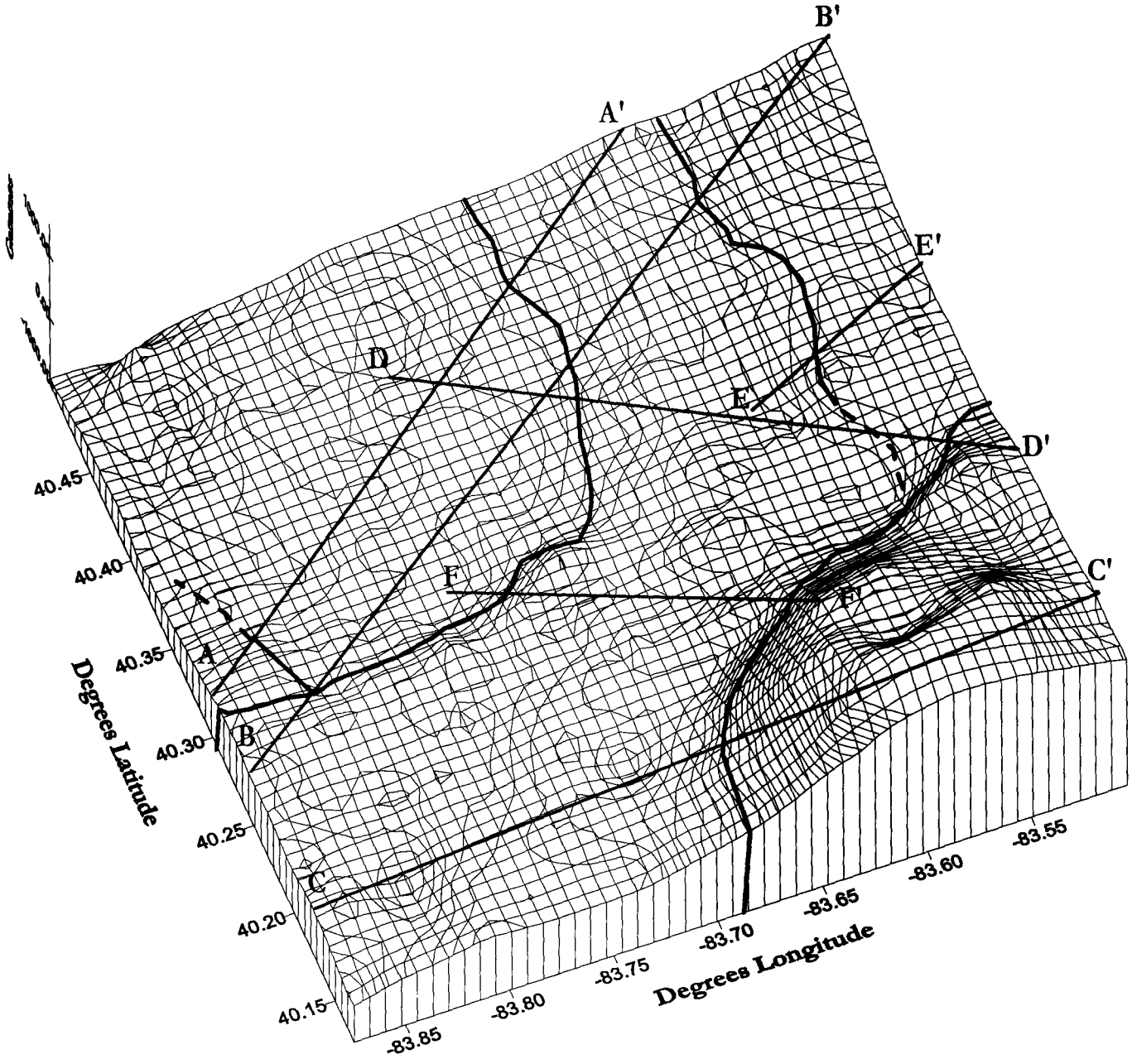

Figure 26. Fault placement according to CBRA investigation of the Bellefontaine Outlier. Contour interval is 2 mgals. Modified from Steck, 1997.

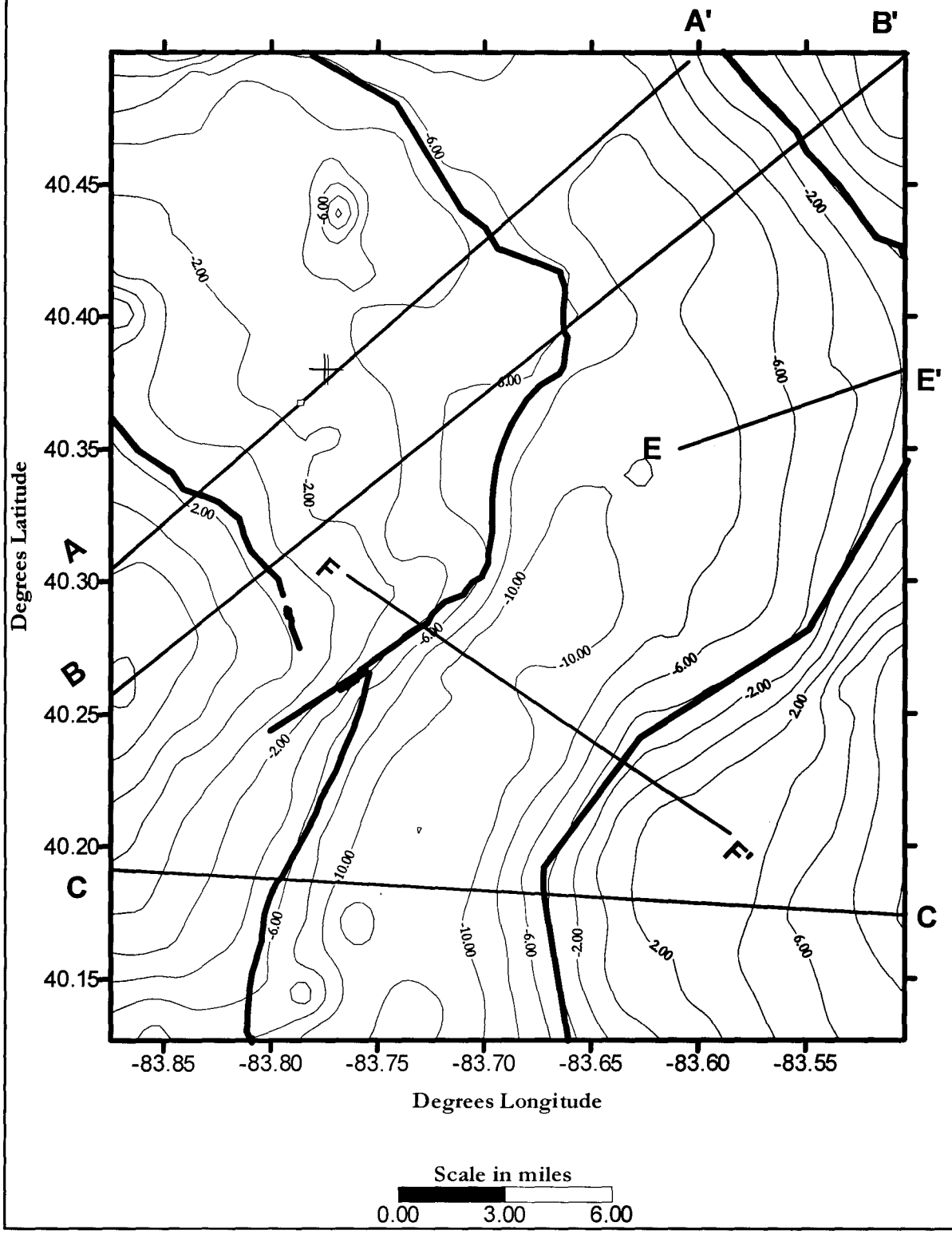

Chapter 4: Conclusions

Investigation of the Bellefontaine Outlier using magnetics has given insight into the basement structure of the region. The general orientation and location of the faults discussed in this senior thesis generally matches those inferred by Steck, 1997 and recent findings of Noltimier et.al., 1998 in ***Basement fault displacement below the Bellefontaine Outlier***. Magnetic anomaly interpretation within this study generally supports these interpretations by Steck, 1997 and Noltimier et. al., 1998. Referring to the magnetic fault anomaly map (see figures 24 and 25) and the gravity fault anomaly map by Steck (see figure 26), some similarities in basement structure are noticeable. There were a few key differences in the placement and number of faults. Fault throws were calculated for the profiles and it was found that they didn't agree with Steck's. This is due to the inherent differences between gravity and magnetics. Steck's 1997 map of faults located by gravity has three major faults within the study area. My fault map identified by magnetics only has two definite faults and one that may be a fault or a lithologic boundary.

The basement of the Bellefontaine Outlier is interpreted to be a reverse graben structure. This reverse graben is bounded on all sides by high angle normal faults that are similar in orientation as Steck's 1997 senior thesis and in the paper by Noltimier et. al., 1993. The central block of the reverse graben is upthrown, resembles a backward s-shape and trends predominantly northeast southwest.

The western border of the central backward s-shaped block is demarcated by a high angle normal fault. A fault, which trends predominately northeast southwest, is located in the central northwest of the study area. It is identified from the magnetic anomaly profiles as faults A-2, B-2, D-1, F-1 and B-1. The fault block west of the fault is downthrown. The fault throw along this fault ranges from 0.38 km at fault A-2 to 0.97 km at fault F-1. It would appear form Table B that the general trend of the fault throw

along this faulted surface increases form northeast to the southwest. This may also suggest that the fault blocks may be off cantered with respect to one another. That is to say one side of the block may be higher than the other.

The northwestern upthrown fault block is interpreted to be faulted by a smaller northwest-southeast trending fault. This fault is identifiable from the magnetic profiles as faults A-1 and B-1, and it is my opinion that this fault makes a junction with fault B-1. This could be from secondary cracking that occurred while the central graben feature

Table 3

Comprison of fault throws derived from gravity and magnetic anomaly interpretation.

Fault #	Throw by Magnetics (km)	Throw by Gravity (km)
A-1	0.08	0.076
A-2	0.38	0.31
B-1	0.13	0.15
B-2	0.37	0.23
B-3	0.87	4.7
C-1	[redacted]	N/a
C-2	N/a	[redacted]
D-1	0.37	0.91
D-2	1.95	1.43
E-1	0.76	N/a
F-1	0.97	0.91
F-2	2.27	1.45

***Highlighted fault throws indicate that they are identical faults and that they were labelled different because there may not have been another fault identifiable on the profile.**

formed. The fault block west of this fault is upthrown, to the east the block is downthrown. The fault throw along this fault ranges from 0.13 km at fault B-1 to 0.08 km at fault A-1. It seems that this fault may actually be incomplete and fails to the north.

The eastern side of the central down dropped block is bordered by a major fault. This fault trends north south, and may extend from the northern border of the study area to the southern border. This fault is identifiable from the magnetic anomaly profiles as faults B-3 and E-1. From (see figures 24 and 25) the magnetic fault map it is inferred that the fault extends to the north and would cross profile A as A-4 if it were inside the study area. To the south it is believed to cross profile D near fault D-2 where it joins up with the inferred fault in the southeastern corner of the study area. The block east of this fault is upthrown. Fault throw along this fault range from 0.87 km at B-3 to 0.76 km at E-1.

Southeast of the central block of the graben is the most prominent feature of the magnetic map. This feature is interpreted as either a volcanic plug or an ore body. A fault is inferred from the magnetic fault map (see figures 24 and 25) and magnetic anomaly profiles C, D and F (see figures 20, 21 and 23). The existence of this fault is hard to determine because of the influence of the large positive anomaly in the southeastern corner of the study area. The anomaly could just be due to a lithologic change. However, it seems likely that the magnetic body is bordered by a fault. It is unknown if the fault formed during the emplacement of the magnetic body, or if the body formed secondary to the faulting. This fault is demarcated in magnetic anomaly profiles as faults C-1, F-2 and D-2. Fault throw along this fault ranges from 2.60 km at fault C-1 to 1.95 km at fault D-2.

It is interesting to note that the magnetic body may actually be an ore body rather than a volcanic plug. Regional drill core has turned up significant amounts of pyrohotite in them. It seems likely that this body may be a pod of ore of significant size. It is unknown as to the size and depth of this body (Personal communication with Noltimier, 1998). Further investigation of this topic is needed to answer these questions.

References Cited

Drahovzal, J.A., Harris, D.C., Wickstrom, L.H., Walker, D., Baranoski, M.T., Keith, B. Furer, L.C., 1992, The East Continent Rift Basin: A New Discovery: Ohio Division of Geological Survey Information Circular 57, 25p.

Hansen, M.C., 1996, The Geology of Ohio-The Precambrian: Ohio Geology, Winter 1996, p. 1, 3-6.

Hansen, M.C., 1991, Campbell Hill-Ohio's Summit: Ohio Geology, Winter 1991, p.1, 3-5.

Hansen, M.C., 1989, "How the World was Made"-The COCORP Traverse of Ohio: Ohio Geology, Winter 1989, p. 1-4.

Hoffman, P.F., 1988, Unied plates of America, the birth of a craton: American review of Earth and Planet Science, v. 16.

Lucius, J.E., Von Frese, R.R.B., 1988, Aeromagnetic and gravity anomaly constraints on the crustal geology of Ohio: Geological Society of America Bulletin, v. 100, no. 1, p. 104-116.

Noltimier, H.C., Steck, S.D, Kaltenbach, K.J., Wickstrom, L.J., 1998, Basement fault displacement below the Bellefontaine Outlier, Logan, Champaign and Logan Counties, Ohio, Interpreted from a 9 quadrangle gravity and magnetic anomaly survey and the Ohio COCORP profile, GSA 1998 North Central Annual Meeting, Columbus Abst. With programs, BTH 21, A-1022, p 64, 1998.

Noltimier, H.C., 1997, Earth physics 680 class notes: Geology 680, Autumn 1997, The Ohio State University.

Noltimier, H.C., 1997, Paleomagnetism 784 class notes: Geology 784, Spring 1997, The Ohio State University.

Pratt, T., Culotta, R., Hauser, E., Nelson, D., Brown, L., Kaufman, S., Oliver, J., and Hinze, W., 1989, Major Proterozoic basement features of the eastern Mid-continent of North America revealed buy recent COCORP profiling: Geology, v. 17, p. 505-509.

Steck, S.D., 1997, Correlation of gravity anomalies with Precambrian crystalline basement, Bellefontaine Outlier, Ohio: Columbus, Ohio State University, B.S. Thesis, 50 p.

Steck, S.D., Wickstrom, L.H., Hansen, M.C., Swinford, E.M., Noltimier, H.C., 1997, Structural evolution of the Bellefontaine Outlier, Ohio: Ohio Geological Society, Fifth Annual Technical Symposium, p. 103.

Telford, W.M., L.P. Geldart, R.E. Sheriff, and D.A. Keys, Applied Geophysics, Cambridge University Press, Cambrige 1976.

Weaver, J.P., 1994, A detailed gravity and magnetic survey of the Bellefontaine Outlier, Logan County, Ohio: Columbus, Ohio State University, M.S. Thesis, 171 p.

Wickstrom, L.H., 1990, A new look at Trenton (Ordovician) structure in northwestern Ohio: Northeastern Geology, v.12, no. 3. P. 103-113.

Wilson, T., 1997, Tectonics 690 class notes: Geology 690, Winter 1997, The Ohio State University.

Appendix

List of magnetic and field station location data. Includes latitude and longitude of the field stations, and magnetic field value in gammas.

Longitude	Latitude	gammas
-83.8397	40.4997	-1135
-83.8386	40.4919	-646
-83.8444	40.4831	-729
-83.8369	40.4817	-640
-83.8586	40.4697	-791
-83.8403	40.4706	-668
-83.8339	40.4656	-885
-83.8114	40.4656	-589
-83.8078	40.4525	-638
-83.8125	40.4836	-616
-83.7653	40.4906	-595
-83.7633	40.4775	-467
-83.7606	40.4594	-465
-83.7592	40.4517	-439
-83.7814	40.4386	-558
-83.7933	40.4378	-614
-83.8050	40.4372	-520
-83.7900	40.4553	-582
-83.8653	40.4417	-715
-83.8542	40.4419	-785
-83.8347	40.4444	-687
-83.8308	40.4500	-758
-83.8306	40.4456	-783
-83.8078	40.4481	-589
-83.7564	40.4336	-491
-83.8514	40.4247	-730
-83.8403	40.4253	-639
-83.8272	40.4275	-624
-83.8092	40.4219	-575
-83.8031	40.4233	-547
-83.7967	40.4300	-492
-83.7542	40.4183	-477
-83.7708	40.3817	-616
-83.7514	40.3900	-514
-83.7703	40.3947	-485
-83.7697	40.4036	-498
-83.7753	40.4136	-494
-83.7731	40.4139	-513
-83.7856	40.3847	-533
-83.7892	40.3850	-593
-83.7892	40.3886	-520
-83.7975	40.3969	-571
-83.7931	40.3928	-525

Longitude	Latitude	gammas
-83.8717	40.3900	-795
-83.8717	40.3750	-693
-83.8481	40.3889	-668
-83.8478	40.3958	-621
-83.8286	40.3886	-597
-83.8708	40.4044	-688
-83.8703	40.4111	-604
-83.8461	40.4092	-624
-83.8306	40.4078	-622
-83.8317	40.4153	-676
-83.7428	40.4992	-390
-83.7411	40.4914	-389
-83.7358	40.4739	-474
-83.7286	40.4786	-464
-83.7308	40.4642	-538
-83.7181	40.4656	-445
-83.7100	40.4758	-446
-83.6994	40.4947	-321
-83.7217	40.4558	-518
-83.7181	40.4386	-407
-83.6850	40.4772	-304
-83.6742	40.4781	-291
-83.6578	40.4986	-303
-83.6439	40.4878	-271
-83.6522	40.4794	-234
-83.6544	40.4775	-268
-83.6314	40.4833	-207
-83.6286	40.4633	-193
-83.6356	40.4625	-256
-83.6403	40.4622	-244
-83.6314	40.4461	-244
-83.6578	40.4619	-288
-83.6544	40.4444	-338
-83.7667	40.4400	-553
-83.7369	40.4358	-573
-83.7428	40.4192	-361
-83.7481	40.4058	-490
-83.7475	40.4022	-481
-83.7264	40.4017	-465
-83.7167	40.3917	-512
-83.6972	40.3956	-405
-83.7008	40.4133	-355
-83.7036	40.4183	-362
-83.7036	40.4267	-450
-83.6997	40.4314	-375
-83.6639	40.4286	-334
-83.6639	40.4150	-342
-83.6603	40.4106	-283
-83.6592	40.4064	-329
-83.6447	40.4069	-284
-83.7050	40.3758	-462

Longitude	Latitude	gammas
-83.6781	40.3778	-371
-83.6744	40.3764	-347
-83.6572	40.3750	-222
-83.6369	40.3792	-94
-83.6767	40.3975	-366
-83.6586	40.4008	-355
-83.6594	40.3917	-295
-83.6431	40.3931	-290
-83.6164	40.4678	-92
-83.6211	40.4928	-95
-83.5969	40.4956	11
-83.5731	40.4969	-19
-83.5772	40.4878	-9
-83.5772	40.4786	58
-83.5447	40.4711	108
-83.5461	40.4892	177
-83.5322	40.4906	133
-83.5189	40.4925	370
-83.5100	40.4750	363
-83.5292	40.4733	212
-83.5903	40.4494	-78
-83.5792	40.4681	45
-83.5694	40.4683	89
-83.5678	40.4522	51
-83.5422	40.4536	149
-83.5114	40.4622	277
-83.5036	40.4567	310
-83.6217	40.4278	-189
-83.5947	40.4397	-145
-83.5669	40.4417	44
-83.5642	40.4333	73
-83.5978	40.4300	-102
-83.5042	40.3944	109
-83.5203	40.3947	28
-83.5086	40.4161	101
-83.5419	40.4244	86
-83.5314	40.4356	140
-83.5453	40.3800	84
-83.6008	40.3758	-126
-83.6050	40.3833	-151
-83.6050	40.3919	-162
-83.5883	40.3911	-60
-83.5669	40.3953	-31
-83.5822	40.4094	-152
-83.5856	40.4097	-123
-83.6164	40.4103	-171
-83.8708	40.3725	-746
-83.8683	40.3639	-699
-83.8569	40.3669	-677
-83.8697	40.3528	-688
-83.8722	40.3458	-645

Longitude	Latitude	gammas
-83.8508	40.3594	-578
-83.8500	40.3661	-706
-83.8406	40.3656	-686
-83.8347	40.3656	-657
-83.8264	40.3653	-669
-83.7933	40.3514	-523
-83.8108	40.3661	-576
-83.8119	40.3500	-613
-83.7992	40.3489	-587
-83.7953	40.3344	-513
-83.8517	40.3447	-622
-83.8419	40.3444	-597
-83.8411	40.3517	-569
-83.8336	40.3428	-552
-83.8342	40.3322	-558
-83.8739	40.3239	-549
-83.8747	40.3092	-486
-83.8556	40.3078	-421
-83.8542	40.3222	-509
-83.7761	40.3569	-473
-83.7744	40.3556	-507
-83.7761	40.3328	-519
-83.7750	40.3447	-450
-83.7614	40.3175	-473
-83.7875	40.3189	-502
-83.8447	40.3233	-498
-83.8356	40.3222	-515
-83.8306	40.3208	-543
-83.8072	40.3197	-496
-83.7992	40.3111	-505
-83.8086	40.3083	-433
-83.7892	40.3111	-470
-83.7800	40.3031	-418
-83.7689	40.3028	-479
-83.7714	40.2892	-318
-83.7606	40.2886	-366
-83.7578	40.3025	-453
-83.8500	40.3083	-424
-83.8322	40.3067	-413
-83.7772	40.2892	-358
-83.7986	40.2906	-400
-83.8078	40.2911	-404
-83.8131	40.2914	-373
-83.8217	40.2914	-430
-83.8294	40.2919	-456
-83.8306	40.3058	-430
-83.8572	40.2956	-400
-83.8625	40.2944	-366
-83.8638	40.2800	-325
-83.8594	40.2792	-319
-83.8539	40.2789	-309

Longitude	Latitude	gammas
-83.8500	40.2781	-341
-83.8400	40.2858	-339
-83.8525	40.2942	-384
-83.8400	40.2781	-328
-83.8328	40.2778	-319
-83.8208	40.2764	-343
-83.8211	40.2692	-248
-83.8222	40.2625	-246
-83.8039	40.2689	-283
-83.8036	40.2619	-265
-83.8028	40.2750	-226
-83.8653	40.2656	-287
-83.8656	40.2586	-327
-83.8669	40.2550	-402
-83.8586	40.2647	-254
-83.8317	40.2611	-220
-83.8408	40.2633	-248
-83.7922	40.2606	-218
-83.7844	40.2594	-258
-83.7856	40.2525	-209
-83.7744	40.2525	-184
-83.7567	40.2564	-195
-83.7633	40.2664	-148
-83.7822	40.2747	-236
-83.7753	40.2744	-216
-83.7731	40.2719	-195
-83.7669	40.2722	-165
-83.7633	40.2731	-180
-83.7536	40.2669	-229
-83.7675	40.2800	-176
-83.7483	40.3680	-489
-83.7258	40.3633	-470
-83.7272	40.3489	-417
-83.7333	40.3361	-387
-83.7447	40.3386	-447
-83.7425	40.3481	-426
-83.7064	40.3650	-475
-83.7211	40.3722	-451
-83.7119	40.3453	-459
-83.7078	40.3525	-425
-83.7142	40.3308	-349
-83.7147	40.3222	-298
-83.7153	40.3175	-364
-83.7300	40.3239	-358
-83.7411	40.3281	-458
-83.6758	40.3442	-291
-83.6750	40.3500	-283
-83.6569	40.3736	-240
-83.6564	40.3558	-278
-83.6361	40.3650	-140
-83.6625	40.3278	-149

Longitude	Latitude	gammas
-83.6342	40.3189	-8
-83.6300	40.3003	-134
-83.6406	40.2953	-25
-83.6294	40.2906	100
-83.6614	40.2994	-156
-83.6672	40.2997	-124
-83.6842	40.2969	-119
-83.6889	40.3219	-291
-83.7036	40.3058	-40
-83.7019	40.3097	-166
-83.7128	40.2989	-42
-83.7272	40.2858	-28
-83.7314	40.2981	-251
-83.7342	40.3053	-351
-83.7369	40.3128	-419
-83.7222	40.2703	-280
-83.7264	40.2639	-167
-83.7300	40.2567	-157
-83.7314	40.2511	-224
-83.7175	40.2564	-200
-83.7161	40.2522	-139
-83.7089	40.2581	-122
-83.7008	40.2600	-130
-83.7036	40.2694	-117
-83.7042	40.2775	-267
-83.7056	40.2864	-93
-83.6881	40.2883	-165
-83.6789	40.2764	-92
-83.6781	40.2664	-123
-83.6611	40.2608	-102
-83.6544	40.2522	-53
-83.6333	40.2567	-10
-83.6511	40.2750	36
-83.6397	40.2808	72
-83.6542	40.2833	37
-83.5856	40.3281	-176
-83.6239	40.3414	-85
-83.6161	40.3558	-134
-83.6142	40.3733	-154
-83.5917	40.3564	-88
-83.5828	40.3211	-16
-83.5911	40.3244	-37
-83.6042	40.3261	-84
-83.5764	40.3328	0
-83.5736	40.3300	11
-83.5608	40.3414	223
-83.5647	40.3553	51
-83.5492	40.3669	63
-83.5278	40.3675	55
-83.5114	40.3642	20
-83.5161	40.3489	175

Longitude	Latitude	gammas
-83.5458	40.3444	81
-83.5069	40.2947	159
-83.5100	40.2997	185
-83.5122	40.3022	174
-83.5144	40.3036	170
-83.5197	40.3178	140
-83.5294	40.3281	158
-83.5197	40.3333	117
-83.5639	40.3008	-20
-83.5883	40.2942	-15
-83.6039	40.2856	-8
-83.6086	40.2850	-20
-83.6208	40.2878	3
-83.5967	40.2986	-21
-83.6211	40.3108	36
-83.5964	40.2817	-43
-83.5856	40.2875	-60
-83.6014	40.2777	-30
-83.6056	40.2692	-23
-83.6125	40.2661	67
-83.5878	40.2633	59
-83.5903	40.2578	95
-83.5847	40.2586	40
-83.5808	40.2550	115
-83.5564	40.2656	62
-83.5481	40.2567	440
-83.5283	40.2517	595
-83.5319	40.2592	671
-83.5419	40.2719	229
-83.5578	40.2689	6
-83.5642	40.2758	-43
-83.5489	40.2836	42
-83.5069	40.2744	412
-83.8606	40.1981	-382
-83.8669	40.1994	-424
-83.8664	40.2022	-477
-83.8656	40.2136	-408
-83.8642	40.2281	-313
-83.8633	40.2342	-305
-83.8433	40.2336	-284
-83.8444	40.2264	-249
-83.8361	40.2183	-343
-83.8169	40.2175	-404
-83.8156	40.2317	-282
-83.8139	40.2458	-277
-83.8322	40.2489	-290
-83.8039	40.2461	-286
-83.7947	40.2467	-225
-83.7847	40.2483	-187
-83.7758	40.2467	-362
-83.7778	40.2219	-278

Longitude	Latitude	gammas
-83.7614	40.2217	-188
-83.7544	40.2483	-228
-83.7506	40.2358	-170
-83.7975	40.2239	-241
-83.7969	40.2306	-273
-83.7981	40.2164	-240
-83.8083	40.2167	-300
-83.8183	40.2106	-301
-83.8375	40.2111	-329
-83.8378	40.2050	-348
-83.8392	40.1914	-383
-83.8203	40.1889	-417
-83.8133	40.1886	-315
-83.7806	40.1944	-220
-83.7794	40.2017	-265
-83.7619	40.1917	-148
-83.7622	40.1847	-179
-83.7639	40.1711	-88
-83.7822	40.1722	-188
-83.7847	40.1578	-175
-83.7994	40.1586	-190
-83.8133	40.1736	-304
-83.8317	40.1747	-497
-83.8411	40.1753	-420
-83.8592	40.1767	-282
-83.8608	40.1692	-264
-83.8619	40.1567	-350
-83.8733	40.1342	-510
-83.8431	40.1569	-318
-83.8531	40.1494	-354
-83.8547	40.1328	-316
-83.8369	40.1314	-260
-83.8108	40.1294	-110
-83.7792	40.1281	-167
-83.7828	40.1447	-212
-83.8131	40.1586	-191
-83.8147	40.1564	-256
-83.8161	40.1406	-209
-83.8333	40.1550	-371
-83.8350	40.1461	-305
-83.7064	40.2233	-62
-83.7100	40.2189	-97
-83.7292	40.2203	-107
-83.7281	40.2356	-116
-83.7286	40.2453	-131
-83.7078	40.2289	-38
-83.6953	40.2314	-44
-83.6958	40.1878	-14
-83.7114	40.2403	-82
-83.7003	40.2425	-125
-83.6953	40.2433	48

Longitude	Latitude	gammas
-83.6892	40.2439	-59
-83.6650	40.2494	-62
-83.6689	40.2372	6
-83.6650	40.2361	24
-83.6611	40.2236	-81
-83.6592	40.2203	-26
-83.6819	40.2150	-71
-83.6569	40.2125	152
-83.6494	40.2081	310
-83.6342	40.2094	542
-83.6442	40.2322	20
-83.6439	40.2361	135
-83.6281	40.2461	178
-83.6500	40.2397	136
-83.7022	40.1878	-84
-83.7106	40.2042	-173
-83.7392	40.2058	-73
-83.7092	40.2111	-89
-83.7014	40.2108	-111
-83.6911	40.2119	-85
-83.6694	40.2092	-31
-83.6850	40.2347	-31
-83.6672	40.2031	105
-83.6625	40.1994	269
-83.6511	40.1925	530
-83.6708	40.1844	262
-83.6789	40.1831	120
-83.6811	40.1869	41
-83.6750	40.1931	130
-83.7114	40.1889	-194
-83.7194	40.1917	-275
-83.7411	40.1939	-101
-83.7419	40.1914	-120
-83.7425	40.1842	-88
-83.7425	40.1697	-98
-83.7342	40.1689	-81
-83.7142	40.1722	-63
-83.6911	40.1803	2
-83.6372	40.1814	880
-83.6267	40.1775	1055
-83.6314	40.1681	1007
-83.6472	40.1739	839
-83.6681	40.1653	369
-83.6850	40.1606	241
-83.7258	40.1544	-55
-83.7361	40.1542	-64
-83.7461	40.1556	-109
-83.7369	40.1431	-187
-83.7289	40.1308	-141
-83.6947	40.1458	56
-83.6972	40.1550	46

Longitude	Latitude	gammas
-83.6822	40.1542	261
-83.6711	40.1558	377
-83.6470	40.1522	794
-83.6336	40.1525	1070
-83.6361	40.1419	1099
-83.6308	40.1414	1164
-83.6328	40.1267	864
-83.6456	40.1392	842
-83.6494	40.1400	741
-83.6778	40.1356	248
-83.6744	40.1278	298
-83.6800	40.1456	272
-83.7089	40.1419	47
-83.6106	40.1975	823
-83.6147	40.2125	787
-83.6186	40.2206	575
-83.6128	40.2392	250
-83.5925	40.2489	201
-83.5897	40.2375	350
-83.5781	40.2233	645
-83.5864	40.2217	727
-83.5747	40.2128	755
-83.5461	40.2383	410
-83.5600	40.2319	514
-83.5703	40.2417	351
-83.5353	40.2481	464
-83.5236	40.2281	481
-83.5153	40.2303	640
-83.5211	40.2417	590
-83.5239	40.2469	595
-83.5036	40.2497	580
-83.5286	40.2197	553
-83.5389	40.2094	645
-83.5572	40.2194	632
-83.5342	40.2025	668
-83.5175	40.1889	789
-83.5078	40.2014	710
-83.5294	40.1431	1079
-83.5064	40.1514	882
-83.5050	40.1706	913
-83.5283	40.1558	1040
-83.5572	40.1917	919
-83.5461	40.1800	1181
-83.5606	40.1739	1184
-83.5600	40.1633	1347
-83.6083	40.1664	1173
-83.6139	40.1761	1042
-83.5978	40.1711	989
-83.5850	40.1792	950
-83.5814	40.1814	921
-83.5956	40.2011	875

Longitude	Latitude	gammas
-83.5850	40.1567	1468
-83.5911	40.1572	1372
-83.6142	40.1664	1157
-83.6022	40.1558	1367
-83.6017	40.1469	1508
-83.6153	40.1550	1289
-83.6000	40.1292	1264
-83.5778	40.1317	1347